

Carbon Cycle Extremes Accelerate Weakening of the Land Carbon Sink in the Late 21st Century

Bharat Sharma^{1,2}, Jitendra Kumar³, Auroop R. Ganguly¹, and Forrest M. Hoffman^{2,4}

¹Sustainability and Data Sciences Laboratory, Department of Civil and Environmental Engineering, Northeastern University, Boston, Massachusetts, USA

²Computational Sciences & Engineering Division and the Climate Change Science Institute, Oak Ridge National Laboratory, Oak Ridge, Tennessee, USA

³Environmental Sciences Division, Oak Ridge National Laboratory, Oak Ridge, Tennessee, USA

⁴Department of Civil and Environmental Engineering, University of Tennessee, Knoxville, Tennessee, USA

Correspondence: Bharat Sharma (bharat.sharma.neu@gmail.com)

Abstract. Rising atmospheric CO₂ enhances the vegetation growth through increased carbon fertilization and water-use efficiency. Terrestrial vegetation uptakes more than one-quarter of total carbon emissions and is modulated by regional climate. The increasing surface temperature could lead to enhanced evaporation, reduction in available soil moisture, and frequent droughts and heatwaves. The compound occurrence of such drivers further drives extreme anomalies in vegetation productivity and net land carbon storage. However, the impacts of climate change on the extremes in net biome productivity (NBP) over longer time periods are unknown. Here we show that due to climate warming about 70% of the regions will experience a larger number of negative NBP extremes than positive towards the end of 2100 which could lead to anomalous losses in carbon sink growth. While the most dominant climate driver of NBP extremes is soil moisture, the compound effect of hot, dry, and fire accounts for 50% of total grid cells affected by extremes. In high latitudes, the positive feedback of temperature and NBP weakens towards the end of the 21st century as co-occurrences of hot temperatures and negative NBP extremes increase. Our results show that the frequency of extremes associated with declines in biome productivity is more than gains, especially in tropics. This increased number of negative NBP extremes raises a concern about whether the Earth is capable of increasing vegetation production with growing human population and rising plant material per capita demand for food, fiber, fuel, and building material. The rise in net negative NBP extremes highlight the risk of not only reduction in total carbon uptake capacity but also of conversion of the land to a carbon source.

Short summary

Rising atmospheric CO₂ enhances the vegetation growth through increased carbon fertilization and water-use efficiency. The increasing surface temperature driven by CO₂ of Earth could lead to enhanced evaporation, reduction in available soil moisture, and increases in droughts and heatwaves. The impact of such climate extremes is detrimental to the terrestrial carbon uptake capacity. We investigated the extremes events in net biomass productivity (NBP), a component of the terrestrial carbon cycle and a measure of net carbon storage flux. We found that due to climate warming about 70% of the regions towards the end of

2100 will show anomalous losses in biome productivity than gains. While lack of soil moisture alone causes the largest number
of losses in biome productivity, the compound effect of hot, dry, and fire events drivers 50% of all NBP extremes. A few high
25 latitudinal regions that were net carbon sinks during warm months are expect to show negative temperature sensitivity to NBP
over time. This increased number of negative NBP extremes raises a concern about whether the Earth is capable of increasing
its capacity to increase vegetation production with increasing human population and rising plant material per capita demand
for food, fiber, fuel, and building material.

1 Introduction

The rising anthropogenic carbon emissions (CO_2) are leading to increase in Earth's surface temperature, climate variability and
30 intensification of climate extremes. Terrestrial ecosystems have historically taken up a little over one-quarter of total carbon
emissions, via carbon accumulation in forest biomass and soils (Friedlingstein et al., 2019), and helped constrain increasing
atmospheric CO_2 concentrations. The increase in net terrestrial carbon sink is a result of decline in deforestation, enhanced
vegetation growth driven by CO_2 fertilization and lengthening of growing seasons in high latitudes. The terrestrial carbon sink
provides negative feedback in the climate-carbon cycle. However, exacerbated environmental changes and climate extremes
35 such as droughts, heatwaves and fires have the potential to reduce regional carbon stocks and carbon uptake (Reichstein et al.,
2013). Net biome production (NBP), one of the components of terrestrial carbon cycle, represents the net carbon uptake
after accounting for carbon losses from plant respiration, autotrophic respiration, fire, and harvest (Bonan, 2015) and is a
critical measure of long-term carbon storage. Climate driven large anomalies in NBP could impact the structure, composition,
40 and function of terrestrial ecosystems (Frank et al., 2015). To improve our understanding of the climate-carbon feedback,
especially during large anomalies, it is important to investigate the changing magnitude, frequency, and spatial distribution of
NBP extremes over long periods and identify the climate drivers at regional and global scales that potentially drive the large
NBP extremes.

The terrestrial carbon cycle processes, such as photosynthesis, respiration and elemental cycling drive the structure, composition and function of the terrestrial ecosystems. In the past few decades, the global terrestrial carbon cycle has taken up
45 25-35 % of the CO_2 emissions from anthropogenic activities such as deforestation and fossil fuel consumption (Piao et al.,
2019). With rising atmospheric carbon dioxide, the carbon uptake by both ocean and land has also increased but with significant
variability over land (Friedlingstein et al., 2019). Since 1980, large interannual variation in the atmospheric CO_2 growth
rate and land carbon are correlated and driven by large-extent climate extremes and lower carbon sequestration (Piao et al.,
2019).

50 The climate extremes are part of Earth's climatic variability affecting terrestrial vegetation and modifying ecosystem-atmosphere feedback (von Buttlar et al., 2018). A number of recent studies have investigated the influence of global warming on
climate extremes and terrestrial ecosystem (von Buttlar et al., 2018; Diffenbaugh et al., 2017; Frank et al., 2015; Zscheischler
et al., 2018). The observations and climate models suggest that global warming has increased the severity and occurrence of
hottest month, hottest day, driest and wettest periods (Diffenbaugh et al., 2017). Heavy precipitation or lack thereof could have

55 negative feedback on the carbon cycle via soil water-logging and drought stress, respectively (Reichstein et al., 2013). A few studies have investigated the impact of climate extremes on the carbon cycle and found that hot and dry extremes reduce the carbon uptake, especially in low latitudes and arid/semi-arid regions (Pan et al., 2019; Frank et al., 2015). The attribution studies infer that the compound effect of multiple climate drivers have a larger effect on carbon cycle and extremes (Zscheischler et al., 2018; Pan et al., 2019; Frank et al., 2015; Reichstein et al., 2013) than any individual climate driver. Most attribution methods focus on analyzing response of carbon cycle to climate, aggregated over annual, sub-annual, and seasonal scales, however, the responses may vary at shorter time scales of daily to monthly.

60 The variability in climate-carbon feedbacks is dependent on geographical location, among other factors. Grose et al. (2020) reported that while Australia is expected to experience an overall reduction in precipitation by 2100, spatial distribution varies as a few regions are expected to get higher and others will receive less precipitation. Ault (2020) found that despite the overall 65 increase in precipitation and water use efficiency globally, the available soil moisture is reducing across many regions due to increased evapotranspiration from higher temperature exceeding the supply from precipitation. The regions that see a decrease in supply and increase in demand for water are sensitive to even low levels of rising temperatures. These feedbacks will increase the severity of droughts and ENSOs will further amplify the effect (Ault, 2020). The net primary productivity (NPP) sensitivity to temperature is negative above 15°C and positive below 10°C (Pan et al., 2019), which means warming will cause a reduction 70 in carbon uptake in tropics and extra-tropics and an increase in carbon uptake at higher latitudes. However, with increasing average surface temperatures, the NPP sensitivity could turn negative over time in high latitude regions.

75 The rising CO₂ and global warming could have implications for biological (Frank et al., 2015) and ecological systems as the severity and occurrence of climate extremes, such as heatwaves, droughts, and fires, are likely to strengthen in the future. These systems are more sensitive to climate and carbon extremes than gradual climate change. Increasing frequency and magnitude of climate extremes could lead to reduction in carbon uptake in tropical vegetation, reduce crop yield (Ribeiro et al., 2020), and negate the expected increase in carbon uptake (Reichstein et al., 2013). In this study we investigated the extremes in the NBP and their climate drivers during 1850 – 2100 across several regions around the globe. The objectives of this study were 1) to quantify the magnitude, frequency, and spatial distribution of NBP extremes, 2) attribute individual and compound climate drivers of NBP extremes at multiple time lags, and 3) investigate the changes in climate-carbon feedback at the regional scales.

80 2 Methods

2.1 Data

We used the Community Earth System Model (version 2), CESM2, simulations at 1° × 1° spatial and monthly temporal resolution to analyze the climate driven extreme events in the net biome production. The CESM2 is a fully coupled global climate model comprising of land, atmosphere, and ocean components. The simulations analyzed here were forced with historical 85 (1850–2014) and shared socioeconomic pathway 8.5 (SSP585; 2015–2100) scenarios, wherein atmospheric CO₂ rises from 280 ppm in 1850 to 1150 ppm in 2100 (Danabasoglu et al., 2020). While CO₂ forcing causes temperature to increase and

land-use changes have a slight cooling effect (Lawrence et al., 2019), resulting in an overall increase of about 8°C mean air temperature over the global land surface during 1850–2100.

2.2 Definition and Calculation of Extreme Events

90 The IPCC (Seneviratne et al., 2012) defines extremes of a variable as the subset of values in the tails of the probability distribution function (PDF) of anomalies. Based on the global PDF of NBP anomalies, we selected a threshold value of $q = 5$, such that total positive and negative extremes comprise of 5% of all NBP anomalies (schematic Figure S1). The negative and positive extremes in NBP extremes comprised of NBP anomalies smaller than $-q$ and larger than q , respectively. For any period, while the total number NBP extremes were constant (i.e. 5% of all NBP anomalies), the count and intensity among
95 positive and negative extremes vary depending on nature of the PDF of NBP anomalies.

We computed extremes for every 25 year period from 1850 through 2100 to analyze the changing characteristics of NBP extremes at regional to global scales. For regional analysis, we focused on 26 **SREX** regions (Figure S2) that are defined in the Special Report on Managing the Risks of Extreme Events and Disasters to Advance Climate Change Adaptation (Seneviratne et al., 2012). We analyzed the characteristics of NBP extremes during carbon uptake period when photosynthesis dominates
100 NBP and land is a net sink of carbon ($NBP > 0$) and carbon release period when NBP is dominated by respiration and disturbance processes and land is a net source of carbon ($NBP < 0$) (Marcolla et al., 2020).

The anomalies in NBP were calculated by removing the modulated annual cycle and non linear trend from the time series of NBP at every grid cell. We calculated the modulated annual cycle and non linear trend of NBP using singular spectrum analysis which is a non-parametric spectral estimation method that decomposes a time series into independent and interpretable components of predefined periodicities (Golyandina et al., 2001). The conventional way of computing annual cycle or climatology does not capture the intrinsic non-linearity of the climate-carbon feedback (Wu et al., 2008). The modulated annual cycle, comprised of signals with return period of 12 months and its harmonics, is able to capture varying modulation of seasonality of NBP under rising CO₂ emissions. The non non linear trend comprised of the return periods of 10 years and higher such that the anomalies in the ecosystem and climate drivers capture the effects of the ENSO, which is believed to have a large impact on climate and carbon cycle (Zscheischler et al., 2014; Ault, 2020). Thus, NBP anomalies consists intraannual variability represented by high-frequency signals (<12 months) and the interannual variability (>12 months and <10 years).
110

2.3 Attribution to Climate Drivers

While most studies traditionally attribute the impact of changes in climate on carbon cycle at seasonal to annual time scales, many responses and variability of climate and its impact on carbon cycle happen at shorter daily to monthly time scales (Frank et al., 2015). Some recent studies have performed attribution by comparing the median of the climate driver distribution in a large space-time dimension (Zscheischler et al., 2014; Flach et al., 2020), which may not capture the variability at regional to the grid cell scales. Using linear regression of time-continuous NBP extremes that represent the large intra- and inter-annual variation in NBP with climate anomalies, we quantified the **dominance** (regression coefficient) and **response** (sign of regression coefficient) of climate drivers on large NBP extremes. The NBP extreme events could either occur contiguously
115

120 over time and space or isolated from other events. The long duration time-continuous extreme events have a larger impact on
 the terrestrial ecosystem than time-separated isolated extreme events. We define time-continuous extreme (TCE) events that
 fulfill the following conditions, (i) it must consist of isolated extremes which are contiguous for at least one season length i.e.
 3 months, and (ii) any number of isolated or contiguous extremes can be a part of a TCE event if the gap among such extremes
 is less than season length (i.e. up to 2 months). We assume that gap greater than or equal to season length as a separate TCE
 125 event.

Human activities such as fossil fuel emissions and land use changes modify biogeochemical and biogeophysical processes
 which alter the climate and climate-carbon feedbacks. Large anomalous changes in climate drivers have a strong impact on
 carbon uptake and biome productivity. Here, we attributed NBP TCEs to climate drivers, namely, precipitation ("Prcp"), soil
 130 moisture ("SM"), monthly average daily temperature ("TAS"), and carbon mass flux into atmosphere due to CO₂ emission from
 fire ("Fire"). As the terrestrial vegetation has ingrained plasticity to buffer and push back effects of climate change (Zhang et al.,
 2014), the impact of change in climate driver is often associated with lagged response. Moreover, the strength of the impact of
 climate on NBP is dependent on location, timing, and land cover type (Frank et al., 2015). The linear regression of TCEs in
 NBP and anomalies of every climate driver was performed at all qualifying land grid cells for lags from one to four months. We
 135 assumed that the higher the Pearson Correlation coefficient (ρ) of a climate driver with NBP extremes, the larger is its impact
 on NBP at that location. The attribution based on ρ is used only for those grid cells where the significance value (p) < 0.05.
 The grid cells with at least two negative and positive NBP TCEs each often yielded high correlation coefficients with high
 significance value (p < 0.05), thus this constraint was applied for attribution to climate drivers.

The instantaneous impact (when lag equals zero) of driver anomalies (dri_t) on NBP TCEs (nbp_t) is computed using the
 Equation 1, where N represents the months in TCEs at any grid cell. Attribution based on the lagged response of anomalous
 140 driver anomalies on NBP TCEs is computed using Equation 2, where L represents the number of lagged months. For lags
 greater than one month, we compute the correlation of the average of climate drivers anomalies, $\frac{dri_{t-l}}{L}$ for every time-step in
 the driver anomalies, with nbp_t . The resulting ρ captures the average response of antecedent climatic conditions up to L months
 that drive NBP TCEs.

145 for lag = 0:

$$\rho = \text{corr}(dri_t, nbp_t) \mid t \in N \quad (1)$$

for lag >0:

$$150 \quad \rho = \text{corr}\left(\sum_{l=1}^{l=L} \left(\frac{dri_{t-l}}{L}\right), nbp_t\right) \mid t \in N \quad (2)$$

The direction and strength of the impact of various climate drivers on plant productivity and carbon sink vary with space
 and time. The increased temperature could lead to increased respiration and losses in NBP in tropics and mid-latitudes, but an

increase in temperature could lead to higher photosynthetic activity in higher latitudes. A moderate reduction in precipitation
155 may not severely impact the vegetation productivity, but if accompanied by heatwave could lead to large losses in NBP. We analyzed dominant climate drivers across SREX regions for every 25 year period from 1850 to 2100 to understand the changing characteristics of large spatio-temporal extremes and its drivers across time and space.

The anomalous climate drivers causing NBP extremes may or may not qualify as climate extremes by themselves. A recent study has found that the extreme years of climate and NBP are often not the same, and the compound effect of non-extreme
160 climate drivers could drive an extreme in NBP (Pan et al., 2019). Since the occurrence of a NBP extreme is likely driven by compound effect of multiple climate divers, we identified co-occurring anomalous climatic conditions during and antecedent to NBP extremes to improve our understanding of the interactive compound effect of drivers on carbon cycle. The dominance of climate drivers are usually quantified by correlation coefficient's range of 0.5 – 0.7, we imposed a limit of correlation coefficients > 0.6 and significance values < 0.05 on co-occurring individual climate drivers to qualify as individual or compound drivers
165 of NBP extremes. These constraints reduced the number of extremes attributable to climate drivers, but identified dominant drivers with high confidence.

3 Results and Discussion

3.1 Characteristics of NBP Extremes

The 5th percentile NBP anomalies computed every 25 year period from 1850 to 2100 render threshold trajectories increasing
170 from 140 GgC/month to 220 GgC/month (Figure S3(a)). This 1.5 times increase in threshold values demonstrates the increasing magnitude of anomalies and interannual variability of NBP across the globe. Corresponding time series of intensity of losses and gains in biome productivity were calculated by integrating the negative (NBP anomalies $< -q$) and positive (NBP anomalies $> q$) extremes anomalies. The rate of increase in the magnitude of negative extremes (-834 MgC/month) was larger than the positive extremes (804 MgC/month) (Figure 1) which implies that overtime the net losses in carbon storage during
175 NBP extremes increases.

The changes in NBP are driven by spatial and temporal variations in climate drivers and anthropogenic forcing. During 1850–1874, 24 out of 26 regions were dominated by carbon release period and the total NBP was less than zero (Figure S3(b)). From 1850 through 1960s, there was a net CO₂ influx into the atmosphere likely driven by deforestation and land-use change activities (Friedlingstein et al., 2019) (Figures S3(b) and S5(a)). After the year 1960, the reduction in the rate of deforestation
180 and increase in fossil fuel emission raised the atmospheric CO₂ concentration. Increasing CO₂ fertilization, water-use efficiency, and lengthening of growing seasons enhanced vegetation growth and NBP with a large increase in tropics and northern high latitudes (Figure S4). After 2070, the total NBP reaches its peaks and starts to decline (Figure S3(b)) as the ecosystem respiration exceeds total photosynthetic activity. The tropical region have the largest magnitude of NBP however the rate of increase of NBP reduces after 2050 and the region of Sahel shows an early decline in total NBP after the year 2050. Longer
185 dry spells and intense rains due to changing precipitation patterns in the Mediterranean and subtropical ecosystems are likely to cause higher tree mortality (Frank et al., 2015). Hot temperatures and reduced activity of RuBisCO hindering carboxylation

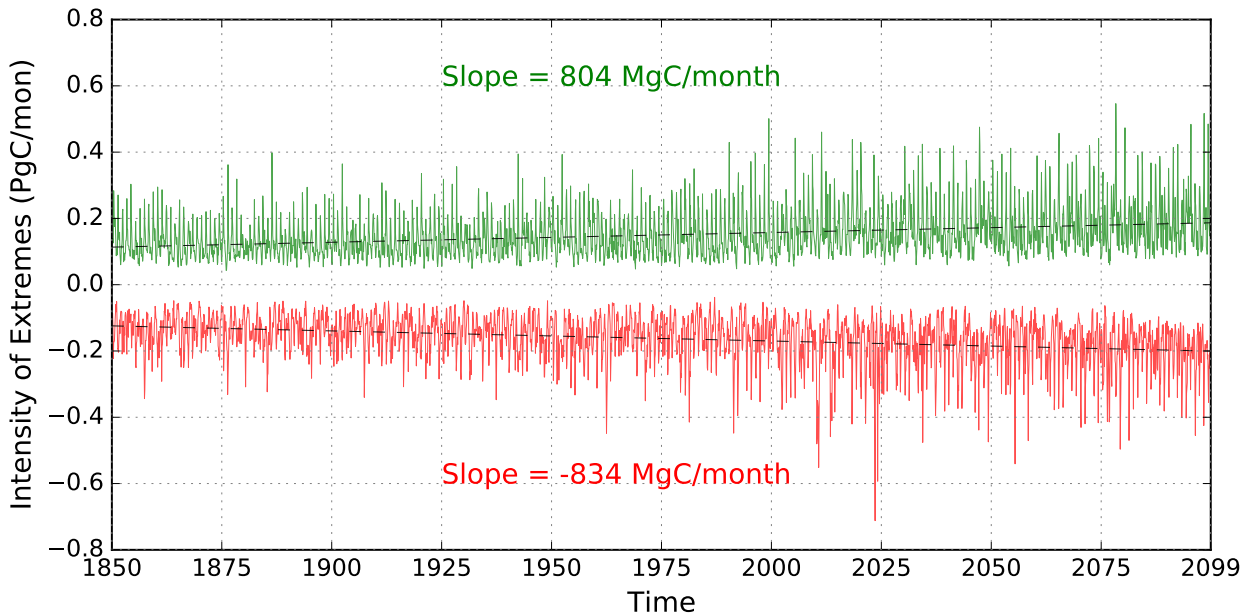


Figure 1. The intensity of positive and negative extremes in NBP in CESM2 are represent by green and red color, respectively. The rate of increase of positive and negative extremes in NBP are 804 and $-834 \text{ MgC per month}$.

are the possible factors that will cause a net decrease in NBP of the region of Sahara (SAH) and make it a net carbon source after 2050. During 2050–74 and 2075–99, the low-latitude regions exhibit the highest regional NBP; however, many regions in the tropics witness a declining growth rate of regional NBP (Figure S4).

190 As anomalous changes in climate vary over space and time, the extremes in NBP also respond to the interactive effects of climate drivers and exhibit spatial and temporal variation. Figure 2 shows net total sum of both positive and negative extremes in NBP in SREX regions integrated for 25 year periods (1850–74, 1900–24, 1950–74, 2000–24, 2050–74, and 2075–99). Most regions exhibit net losses in the biome productivity during extremes, e.g. South Africa (SAF) has always been dominated by negative NBP extremes. The large magnitude of net carbon uptake changes during the period 2000–24 was likely driven by
 195 a change in LULCC forcing from decadal to annual during 2000–2015 and then back to decadal 2015 onward. The change in resolution of LULCC forcing possibly caused higher climate variability due to biogeophysical feedbacks and subsequently led to increased carbon cycle variability and extremes. 23 out of 26 SREX regions experience an overall loss in biomass productivity during extremes during the end of the 21st century (Figure 2). The distribution of the total magnitude and count of negative TCEs during 2075–99 across all the SREX regions follow a similar pattern i.e., more frequent the extremes larger
 200 were the carbon losses (Figure 3(a)). The largest losses in carbon uptake during TCEs were in tropical regions, e.g., East Asia (EAS), Amazon (AMZ), and SAF, with -3, -3, and -2.25 PgC carbon loss during 2075–99. These regions also witness the highest number (1270, 1410, 950) of negative NBP TCEs. The magnitude of carbon losses and the number of negative

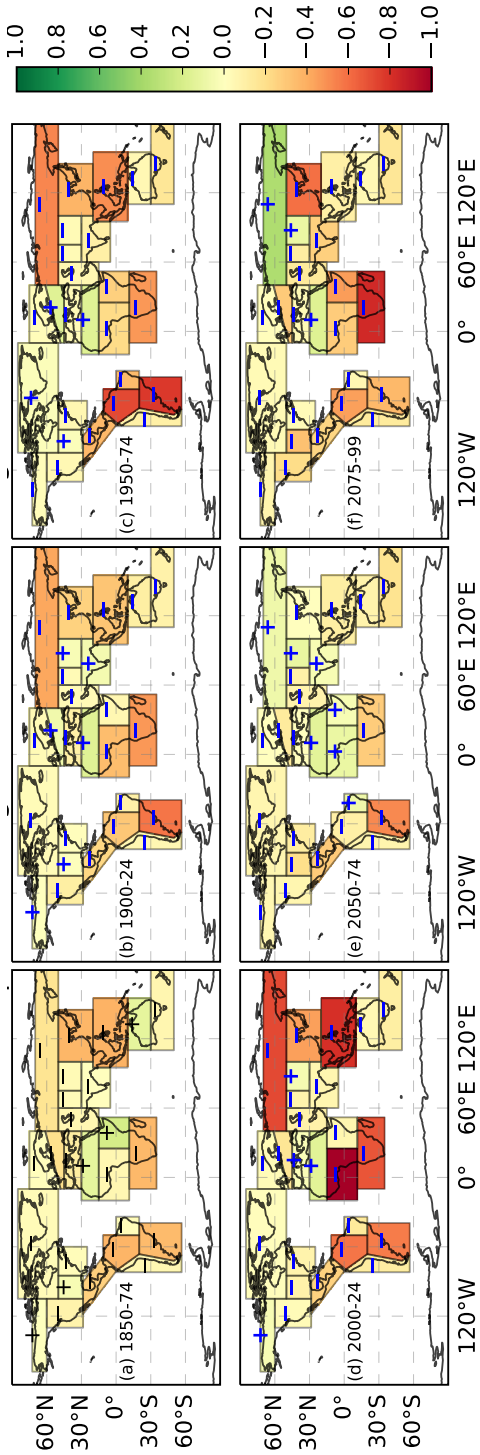


Figure 2. The sum of positive and negative carbon cycle extremes is referred as Net Uptake Change during NBP extremes. The figure shows the changing spatial distribution of net uptake change (PgC) during following periods: (a) 1850–74, (b) 1900–24, (c) 1950–74, (d) 2000–24, (e) 2050–74, and (f) 2075–99. Net gain in carbon uptake is represented by green color and '+' sign; net decrease is represented by red color and '-' sign. At most regions, the magnitude of negative NBP extremes or losses in carbon uptake are higher than positive NBP extremes or gains in carbon uptake.

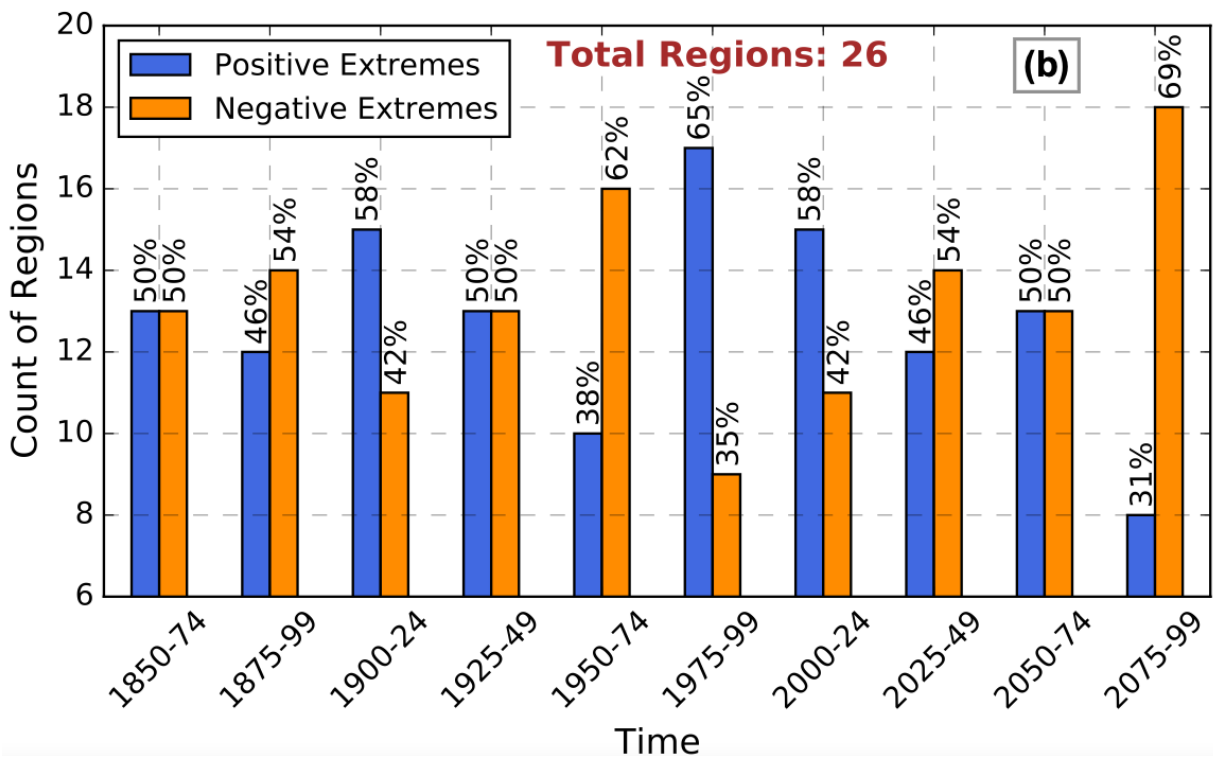
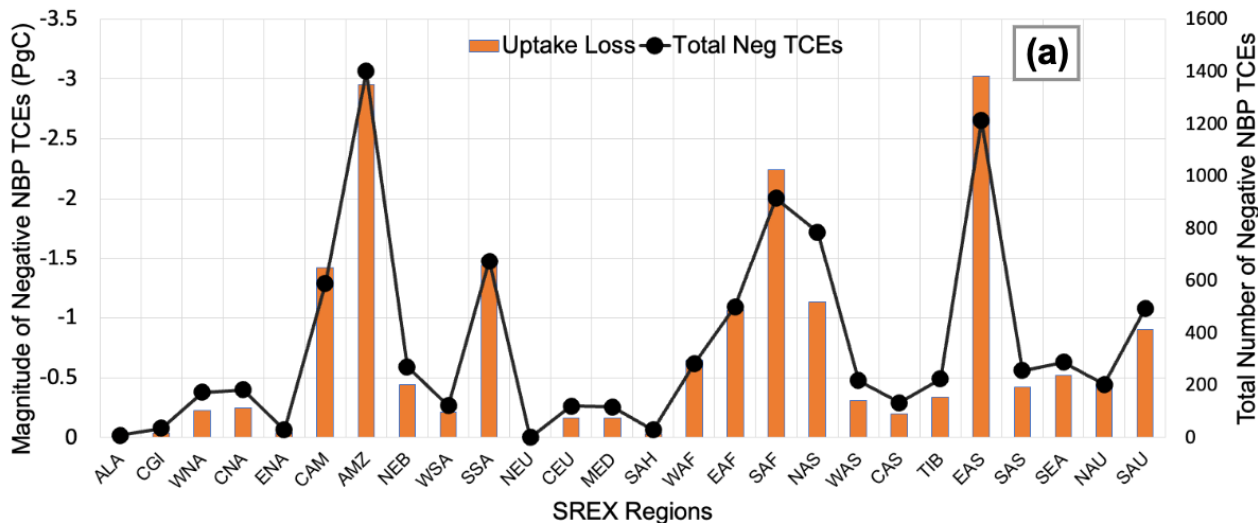


Figure 3. (a) Total magnitude of negative carbon cycle extremes or loss is carbon uptake during TCEs across SREX regions plotted as bar graph (left y-axis). Total number of negative TCE events (right y-axis) plotted as line graph. The largest portion of carbon uptake loss is in tropical SREX regions of Amazon (AMZ), East Asia (EAS), and South Africa (SAF) for the period 2075-99. (b) Count (y-axis) of the regions dominated by either positive or negative NBP extremes. Relative to a total of 26 SREX-regions, the percent count of positive or negative NBP extremes is represented at the top of the bars.

NBP TCEs were highest in tropical regions. The magnitude and number of negative TCEs were very low for high latitude of Alaska(ALA), Canada and Greenland (CGI), Eastern North America (ENA), North Europe (NEU), Central Europe (CEU),
205 and dry regions of Mediterranean (MED) and Sahara (SAH). Although the number of NBP TCEs in NAS are more than Southeastern South America (SSA) and Central America (CAM), the magnitude of NBP TCEs in NAS are low due to less regional NBP. Since the extremes were calculated based on global anomalies in NBP, the largest impact on terrestrial carbon uptake are expected in the regions of AMZ, EAS, and SAF.

The magnitude and the total number of regions dominated by negative extremes in NBP are expected to gradually increase
210 in the 21st century (Figure 3(b)). Most of the increase in the frequency of negative extremes in NBP would occur in ENA, South Asia (SAS), SAF, and CAM (Figure S6). The increase in the magnitude (23 out of 26 or 88% of regions) and frequency (18 out of 26 or 70% of regions) of negative NBP TCEs in most SREX regions during 2075–99 is a matter of concern since the total global NBP peaked at around 2070 and declines further in the model (Figure S3(b)). The negative NBP TCEs dominate in eight out of nine tropical regions, which store the largest standing carbon biomass and represent the largest portion of carbon
215 uptake loss during negative NBP extremes.

The strengthening of negative extremes relative to positive extremes in NBP is of concern to future terrestrial carbon sink capacity as the growth rate of NBP turns negative after around 2070 (Figure S3(b)). A large magnitude of extreme events in the NBP could lead potentially to a state of low and decreasing carbon sink capacity which further lead to positive feedback on climate warming. The positive feedback of warming and climate driver losses in carbon uptake posses many concerns
220 about the implications of reducing terrestrial uptake capacity on food security, global warming, and ecosystem functioning. Moreover, the biological system's sensitivity is higher for climate and carbon extremes than for gradual changes because of larger response strength and shorter response times (Frank et al., 2015).

3.2 Attribution to Climate Drivers

The increase in climate variability and extremes driven by rising CO₂ emissions influence the terrestrial carbon cycle (von
225 Buttlar et al., 2018; Reichstein et al., 2013). Soil moisture was the most dominant climate driver driving the largest number of NBP TCEs (Figure S7). The percent of total number of grid cells which show soil moisture as a dominant driver of NBP extremes were about 40 to 50 percent from 1850 to 2100 across multiple lags, which means that the near term and long term impact of soil moisture were highest among other drivers. The positive correlation of soil moisture anomalies with NBP TCEs indicate that a decline in soil moisture causes a reduction in NBP and vice-versa. Likewise, the dominant climate driver across
230 26 SREX regions was also soil moisture and with positive correlation relationship with NBP TCEs (Figure 4). However, the percent of total number of grid cells dominated by precipitation doubled (10 to 20 percent) when lag was increased from 1 to 3 months. This implies that antecedent declines in precipitation limits carbon uptake more than recent fall in precipitation and possibly causes a decline in soil moisture. Moreover, the plants with deep roots are less impacted with short-term reduction of precipitation than prolonged droughts which are caused by soil moisture limitation. By the end of the 21st century, 70% of the
235 total number of NBP extremes will be water-driven i.e. due to soil moisture and precipitation. Our results were consistent with the recent studies that have found that the most important factor limiting vegetation growth is dryness stress which is caused

mainly by low soil moisture (Liu et al., 2020) and lack of soil moisture for longer periods could result in drought events, causing a larger reduction of ecosystem productivity and smaller reduction of terrestrial respiration (Pan et al., 2019).

The second most important driver of NBP TCEs was fire which was positively correlated (Figure S7). Fire is an important
240 Earth system process that is dependent on vegetation, climate, and anthropogenic activities. CESM2 incorporated a process-based fire model, which contains three components, namely, fire occurrence, fire spread, and fire impact (Li et al., 2013). The interannual variability of agricultural fires is largely dependent on fuel load and harvesting; deforestation fires included fires due to natural and anthropogenic ignitions, caused by deforestation, land-use change, and dry climate. Peat fires usually occur in the late dry season and are strongly controlled by climate. The current version of the fire model reasonably simulates burned
245 area, fire seasonality, fire interannual variability, and fire emissions (Li et al., 2013). As fires are controlled by soil moisture, temperature, and wind, the attribution of NBP extremes to fires could also include the NBP extremes that could be driven by lack of soil moisture and hot temperatures. The anomalies in the fire in the model only include the non-seasonal fires. Therefore, total number of fires events could be larger and recovery after such fire driven extremes could be much longer.

Hot temperatures if persists for long periods causes heatwaves which tend to reduce ecosystem production and enhanced
250 terrestrial respiration causing a large reduction in NBP (Pan et al., 2019). The leaf photosynthesis depends on RuBisCO limited rate of carboxylation which is inversely proportional to the Q_{10} function of temperature (Lawrence et al., 2019). Hubau et al. (2020) found that with increasing temperatures and droughts, the tree growth has been reduced and could offset the earlier gains. On the contrary, warm temperatures in the northern high latitudes cause an increase in carbon uptake due to reduced snow cover and optimal temperature for photosynthesis. Increased warming at northern high latitudes could lead to hot temperature-related
255 hazards and alter temperature-carbon interactions.

Jitu: Next paragraph repeats a lot of points that have been already discussed. The influence of climate drivers on NBP extremes is dependent on the regional interannual variability of climatic conditions and vegetation composition. Low soil moisture and intense fires are the most common causes of negative NBP extremes, for 23 of 26 SREX regions during any time-window (Figure 4). Similarly, positive NBP extremes are driven by increased water availability and optimal temperatures for
260 plant growth. The largest vegetation losses during the NBP extremes are in the tropical forested regions with large above-ground carbon stock (Figure 2). The frequency and magnitude of negative NBP TCEs for period 2075–99 (Figure 3(a)) also highlight the exposure of tropics to NBP extremes. Rising CO₂ emissions drive high temperature in tropics and have the potential to hinder photosynthesis and vegetation growth. The changes in circulation patterns might also influence the precipitation cycle resulting in longer dry spells and could increase fire risks with canopy closure (Frank et al., 2015; Langenbrunner et al., 2019).

The second-largest magnitudes of negative NBP extremes are witnessed by arid and semi-arid regions with mostly grasslands
265 (Figure 3(a)). Several studies conclude that soil moisture causes an increase in dry days and a sizeable negative effect on the carbon cycle driven by increasing droughts in arid, semi-arid, and dry temperate regions (Frank et al., 2015; Zscheischler et al., 2014; Pan et al., 2019). The regions of South Africa, Central America, and Northern Australia witness the largest NBP extremes driven by fire. The region of Amazon was dominated by fire, soil moisture, and temperature in the 21st century. Reduction of
270 fuel load by changing vegetation (PFT) composition could likely be the reason for lesser fire-dominated regions later in the 21st century.

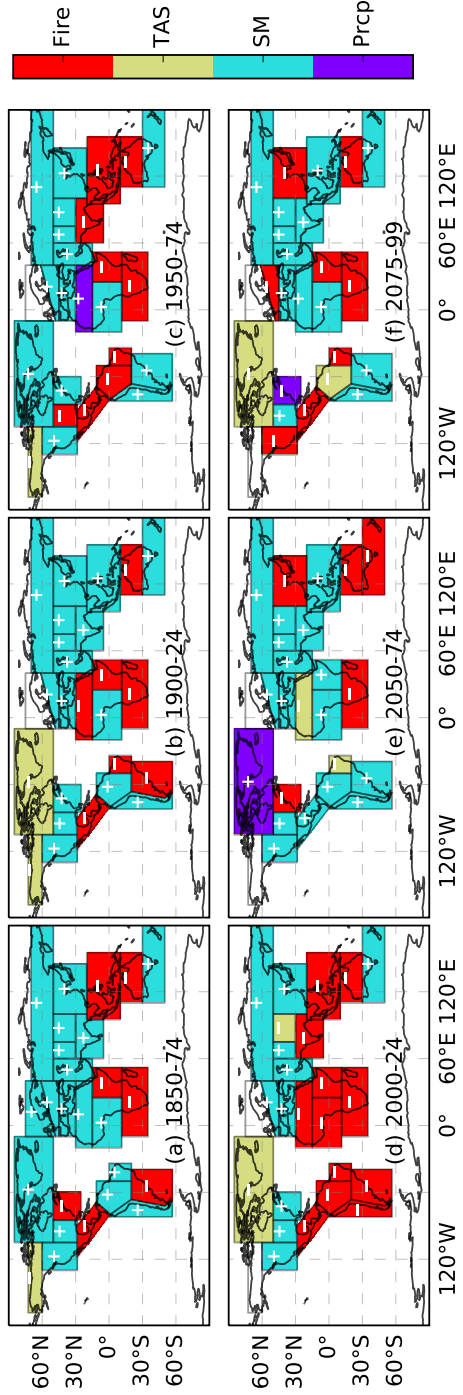


Figure 4. Spatial distribution of dominant climate drivers across SREX regions. The color in every SREX region represents the most climate driver causing carbon cycle extremes at 1 month lag for following periods: (a) 1850–74, (b) 1900–24, (c) 1950–74, (d) 2000–24, (e) 2050–74, and (f) 2075–99. The positive ('+') and negative ('−') sign within a region represents the correlation relationship of NBP extremes with every dominant climate drivers.

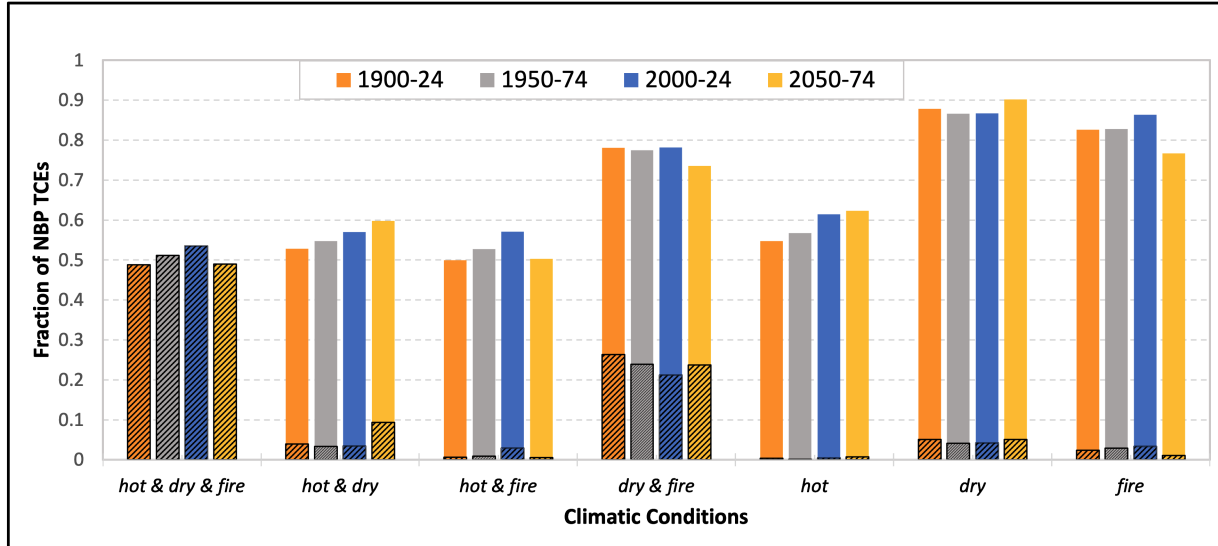


Figure 5. Fractional distribution of carbon cycle time-continuous extremes (TCEs) driven by compound climate drivers at lag of 1 month. The hatched and unhatched bars represent the mutually inclusive and exclusive compound and individual climate drivers, respectively. The exclusive climate drivers are always less than or equal to mutually inclusive drivers. The different colored bar represents following periods: 1900–24, 1950–74, 2000–24, and 2050–74 (*from left to right bar*). Most carbon cycle extremes are driven by interactive effect of climate drivers.

3.3 Compound Effect of Climate Drivers

The interactive effect of multiple climate drivers could lead to devastating ecological consequences as compound extremes often have a larger impact on the carbon cycle than the aggregate response of individual climate drivers (Zscheischler et al., 2018; Ribeiro et al., 2020; Pan et al., 2019). At most grid cells, NBP extremes were either positively correlated with anomalous precipitation and (or) soil moisture, and (or) negatively correlated with temperature and (or) fire. Thus, a negative extreme in NBP was correlated with a decline in precipitation and (or) soil moisture, and (or) increase in temperature and (or) fire events. We used three broad climate driver pools, namely, water (dry or wet), temperature (hot or cold), and fire to study the compound effect of climate drivers.

The largest fraction, about 50%, of total NBP TCEs were attributed to the combined effect of *hot & dry & fire* events (Figure 5). This implies that every other large extreme anomalous event that was associated with huge losses in biomass productivity was driven by the interactive effect of water limitation, hot days (heat waves) and both these drivers could trigger a fire which amplifies the impact on carbon cycle. The second strongest compound driver was *dry & fire* which causes about 25% extremes exclusively. With increasing climate warming, the number of NBP extremes driven by dry climatic conditions have shown a secular increase, with about 10% extremes driven exclusively by *hot & dry* events during 2050–74, contributing 60% to the total NBP extremes were attributed to hot and dry climatic conditions. Although the negative impact of water

limitation (*dry*) on NBP extremes was the highest (90%), rising emissions and climate change will lead to rising number (10% rise) of NBP extremes driven by (*hot*) days.

3.4 Quantifying Changes in NBP Extremes in Tropics

290 Global warming has led to an increase in climate extremes which greatly affect the carbon cycle in tropical forests. Studies using observational data suggest the rate of carbon uptake of Amazonian forests is already declining and in the future carbon uptake will decline in African forests as well (Hubau et al., 2020). With large standing biomass of the planet and carbon uptake in tropics, rise in hot temperatures increases the fire risk and the ecosystem respiration which potentially will cause the growth rate of NBP to flatten out by late 21st century (Figure S5(b)). Further increase in disturbances in the terrestrial carbon cycle will 295 likely result in a large reduction in stored carbon and reversal of tropical carbon uptake to a potential carbon source. Figure 3(b) shows the increasing dominance of negative NBP extremes in SREX regions, where 23 out of 26 SREX regions are dominated by negative NBP extremes during 2074–99. 9 out of 26 SREX regions represent tropical regions which are CAM, AMZ, NEB, WAF, EAF, SAF, SAS, SEA, and NAU (Figure 2). During 2075–99, 8 (except NAU) out of 9 tropical regions were dominated 300 by negative NBP extremes. As the rate of increase of NBP in most tropical regions is either saturating or declining towards the end of the 21st century, increasing frequency of negative extremes possible cause a faster decline in carbon stored in the tropical forests.

The decline in carbon uptake capacity in tropics is primarily driven by rising temperature causing plant mortality due to increase in water stress (lack of soil moisture, increase in evapotranspiration, and strong droughts), changes in circulation, and increase plant respiration (Hubau et al., 2020). The 90th quantile temperature in Central America (CAM) increases from 28°C 305 to 33°C in the 21st century (Figure S8(a)). A similar increase is seen in the 10th and 20th quantile temperatures, which could increase the night time plant respiration and stomatal limitation. Figure S5(a) shows the total carbon loss from natural and managed fire (including deforestation) in the grids cells that witnessed land-use changes in CAM. The large carbon loss due to fires likely led to low NBP of –0.22 PgC/month (Figure S5(b)) during the 1940–1960. After the 1960s, the growth rate of NBP increased due to reduced land-use activities and increased CO₂ fertilization. The total NBP in the region CAM reaches its peak 310 of 0.2 PgC/month around 2060 (Figure S5(b)), which is less than the largest draw down of the region and then declines over time. These patterns raise the risks associated with global warming and consequent decline in carbon uptake and sink capacity.

Towards the end of the 21st century, the frequency of negative NBP extremes exceeds positive extremes (Figure S9(a)) with a larger number of negative extremes than positive occurred during carbon release period (Figure S9(b)). The highest 315 number of negative NBP extremes occur during the periods 1925–49 and 1950–74 which are also the periods when the fire emission from land-use change were maximum (Figure S5(a)). The losses in carbon storage increases when more negative NBP extremes occur during the phase of dominant ecosystem respiration. The strength of negative temperature sensitivity to NBP is also increasing over time (Figure S10), stating that climate change accelerates the reduction in NBP. The negative sensitivity values are gradually increasing from –20 GgC/month·°C (and –30 GgC/month·°C) to –33 GgC/month·°C and 320 (–70 GgC/month·°C) from 1850–60 to 2090–10 for CAM (and AMZ). The region of South-East Asia (SEA) saw the highest negative temperature sensitivity of –207 GgC/month·°C. Similar patterns are seen in other tropical regions that indicate the

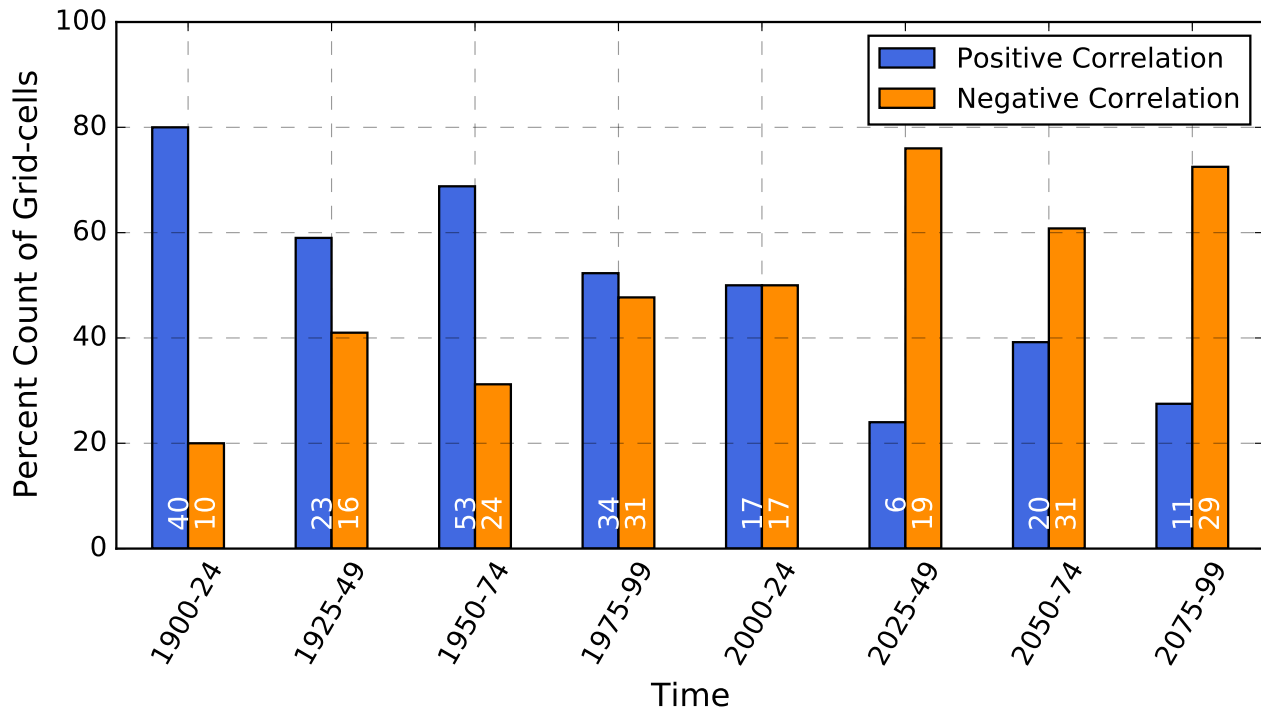


Figure 6. Percent distribution of grid cells with positive and negative correlation of extreme NBP anomalies with temperature (TAS) at a lag of 1 month in the region of Northern Asia (NAS). The blue and orange color bars highlight the positive and negative correlations. The total number of grid cells that experienced NBP extremes and dominated by positive and negative correlations are shown at the bottom of the respected bars.

rise in surface temperatures and increasing negative temperature sensitivity to terrestrial vegetation. Hence, all these factors indicate a possible accelerated reduction in carbon uptake and storage capacity in tropics and significantly impact on the ecological system with the largest standing biomass of the planet.

3.5 Changing Temperature–NBP Responses at High Latitudes

325 The effect of rising temperature on greening and carbon uptake is dependent on the geographical location. Pan et al. (2019) stated that net ecosystem production (NEP) has a negative sensitivity to warming at 81 percent of the global vegetated land area during 2007–18 and only the region at higher latitudes and Tibetan Plateau had a positive sensitivity of NBP to temperature. Marcolla et al. (2020) found a positive sensitivity of NBP to air temperature in higher latitudes and negative sensitivity in tropics. We found that number of NBP extremes in upper-mid and high latitudes represented < 10 % of all global NBP extreme events; the major regions included ALA, CGI, NEU, CEU, and NAS. We found a positive correlation of mean air temperature anomalies and extreme NBP anomalies in higher latitude till 2015, thus validating our findings with existing literature. While the regions of Alaska (ALA), Canada, Greenland, and Iceland (CGI) have a positive correlation of temperature with NBP

anomalies during 1850–2100, the regions of North Asia (NAS), Central Europe (CEU), and Tibetan Plateau (TIB) witness an increasing number of grid cells with a negative correlation of temperature with NBP anomalies over time which means warmer
335 temperatures will cause loss of stored carbon.

Along with the boreal vegetation, above mentioned regions store large underground carbon and exposure to warming and increase in NBP extremes poses a risk of release of stored carbon (Marcolla et al., 2020) into the atmosphere. Increasing number of grid cells with negative correlations of NBP TCEs with temperature in NAS implies that hot temperatures in the future will cause losses in biomass productivity (Figure 6). The 10th quantile temperature increased from -25°C during 1900–
340 24 by 14°C to -11°C during 2075–99. The temperature increased by 8°C of 90th quantile for the same time period. The rate of increase of 10th quantile temperature is 1.7 times higher than 90th quantile temperature in NAS (Figure S8(b)) which could result in increased night time ecosystem respiration and low NBP over time. This rate of warming at high latitudes is much higher than tropics (Figure S5(b)). The long term (10 years average) sensitivity of detrended NBP to detrended surface air temperature is negative for tropical regions and positive for high latitudinal regions (Figure S10); thus, warmer temperatures
345 at high latitudes lead to favorable conditions for plant growth and increase greening. However, at shorter periods, e.g., during 30 month periods, we found that the temperature sensitivity of NBP to temperature is becoming more negative in NAS. The short duration negative temperature sensitivity is possibly causing negative extremes in NBP at high latitudes driven by hot temperatures.

We investigated the co-occurrence of low ($\leq 10^{\text{th}}$ percentile) NBP and hot ($\geq 90^{\text{th}}$ percentile) temperatures in NAS. We
350 found that towards the end of the 21st century, the number of months of co-occurrence of hot temperature with low NBP months increases by about four times compared to 1950–74 (Figure S11). The most dominant months of these co-occurrences are June and July. During summers, most of the high latitudes witness an increase in plant photosynthesis and carbon update. However, with the warming of warm and cold temperatures there is a potential risk of losing a carbon sink and an accelerated release of stored carbon into the atmosphere. The NAS region has also reported a reduction in total NBP during 2075–2099,
355 breaking the consistent increasing trend since 1850. The rising hot temperatures could also increase the thaw rates of permafrost regions under RCP 8.5 (Turetsky et al., 2020) and potentially release carbon dioxide and methane. The saturation of total NBP (especially in tropics) and increasing negative correlated temperature extremes at higher latitudes, poses grave concern for the future of terrestrial ecosystem to act as carbon sink at par with increasing CO₂ concentrations.

4 Conclusions

360 Adverse climatic conditions could lead to fire, droughts, and heatwaves, which could result in huge losses of carbon from stored biomass and possibly convert terrestrial ecosystem into carbon source during the negative NBP extremes. The global growth rate of atmospheric CO₂ and carbon uptake of land and ocean indicate the relative strength of carbon sources and sinks have risen by similar magnitude in the past. However, the dominance of negative NBP extremes and the saturation of NBP towards the end of the 21st century presents a pressing question: To what extent rising temperatures and induced losses in carbon uptake
365 might offset global carbon uptake due to increasing CO₂ and carbon sequestration?

We found that the frequency and intensity of negative extremes in NBP are larger than positive extremes. Since negative NBP extreme events are associated with intense loss of vegetation in short duration, the destruction of vegetation structure and composition is possibly massive and might take longer to recover. The major losses in biomass productivity occurred in tropics, followed by arid and semi-arid regions. After the 1960s, reduction in deforestation and CO₂ fertilization led to an increase in NBP globally until it peaked in 2070 and then NBP starts to decline. However, the magnitude of negative extremes in NBP continues to increase. During 2075–99, 23 out of 26 SREX regions are dominated by negative NBP extreme events, with spatial predominance in the tropical regions. The continuing increase in the magnitude of negative extremes beyond 2100 could further stress vegetation that might lead to a faster decline in stored carbon and potential conversion of the terrestrial ecosystem to net carbon source.

The climate driver causing most NBP extremes is anomalous soil moisture with dominance over 45% of grid cells at multiple lags followed by fire. The number of grid cells dominated by precipitation increases with lag months which shows that decline in precipitation followed by soil moisture possibly leads to negative NBP extremes. Extreme increases in temperature compounded with dry conditions impact vegetation productivity more than the sum of individual climate drivers and could accelerate plant mortality. It also increases the risk and occurrence of fires and compound effect of all three climate drivers causes the largest fraction of NBP TCEs. The compound climate drivers are associated with large anomalous changes in climate conditions in relatively short duration of time which could also impact terrestrial ecosystems, wildlife, and managed croplands which possibly poses a threat to food security, and increase people migration.

The warmer temperature in the northern high latitudes compensates for the loss of carbon uptake in tropical and mid-latitudes due to increased ecosystem respiration driven by hot temperatures in low and mid-latitudes. We found an increasing number of upper-mid latitudinal regions over time where the losses in biomass productivity will be driven by hot temperatures. Though the sensitivity of temperature and NBP are positive in northern high latitudes, we saw numerous short-duration episodes of negative temperature sensitivity to NBP. With an accelerated increase in the surface temperate in the northern high latitudes, carbon release from permafrost melting and the likelihood of reversal of the positive temperature-carbon feedback is increasing over time. Increased negative extremes in NBP and modified climate-carbon feedback in the northern high latitudes could be of grave concern as they store a significant amount of carbon.

Hot temperatures and lack of water availability in tropics are likely to increase terrestrial ecosystem respiration and reduce vegetation growth rate. The frequency of negative extremes is increasing in low latitudes, especially during the carbon release periods. Moreover, the growth rate of NBP is decreasing and negative temperature sensitivity of NBP is strengthening over time. With increasing temperatures, more negative extremes in NBP, and reduced growth of NBP at low latitudes, there is a potential for accelerated reduction in carbon uptake capacity. Large standing carbon stock (fuel load) with hot and dry climate (sources of ignition) increases the fire risk and potential loss of carbon stock during negative NBP extremes.

This study has analyzed climate-driven NBP extremes using the CESM2 model simulation from 1850 to 2100. The future work will use multi-model model analysis to evaluate the agreement among different earth system models of magnitude, frequency, and spatial distribution of NBP extremes and their attribution to the individual and compound climate drivers. The

400 longer-term simulations are needed to analyze the climate-carbon feedback post-2100 when the difference between rate of CO₂
emissions and terrestrial carbon uptake is expected to increase.

Code availability. Data analysis was performed in Python, and the analysis codes will be available on GitHub at https://github.com/sharma-bharat/Codes_NBP_Exremes upon acceptance of manuscript.

Data availability. The selected variables from CESM2 were downloaded from ESGF using the link: [https://esgf-node.llnl.gov/projects/esgf-llnl/](https://esgf-node.llnl.gov/projects/esgf-405_llnl/).

Appendix: Supplementary

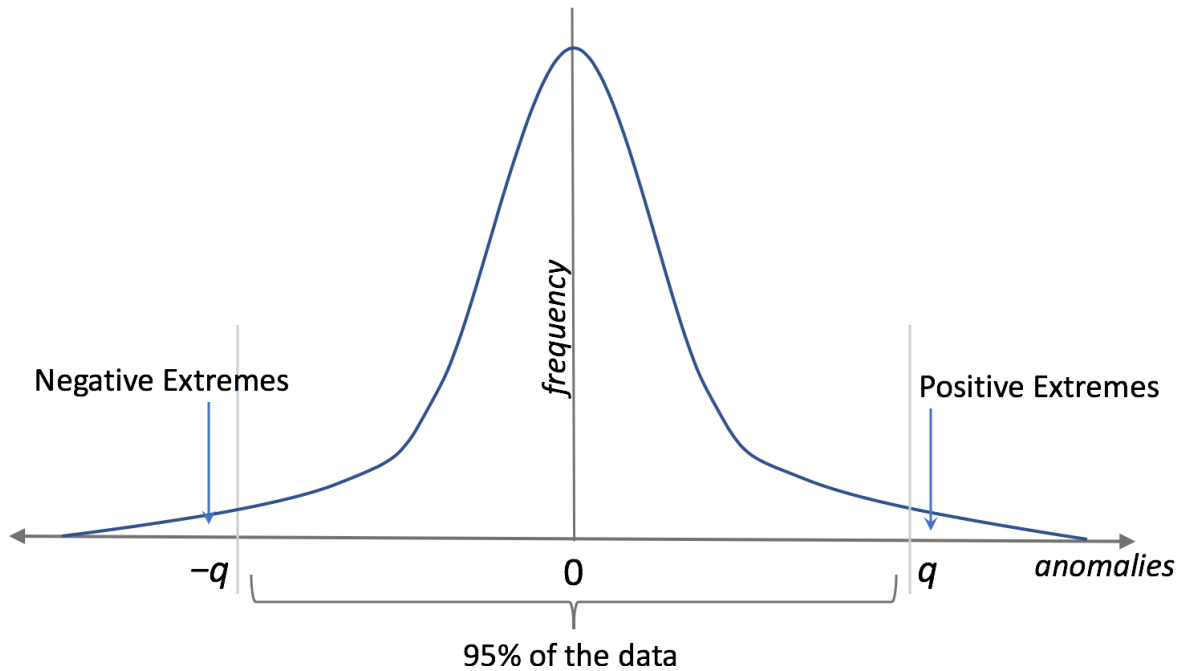


Figure S1. The schematic diagram representing the NBP extremes, that lie in the tails of NBP anomalies. A threshold q is set at 5th percentile in this study, such that 95% of the NBP anomalies lie within $-q$ and q .

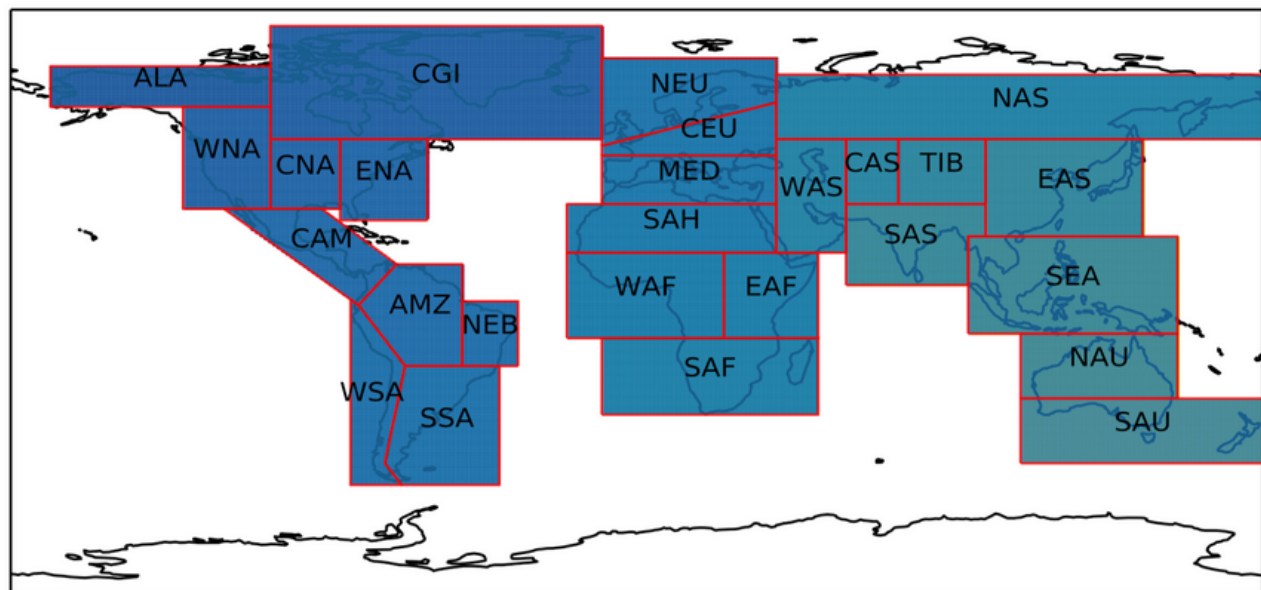
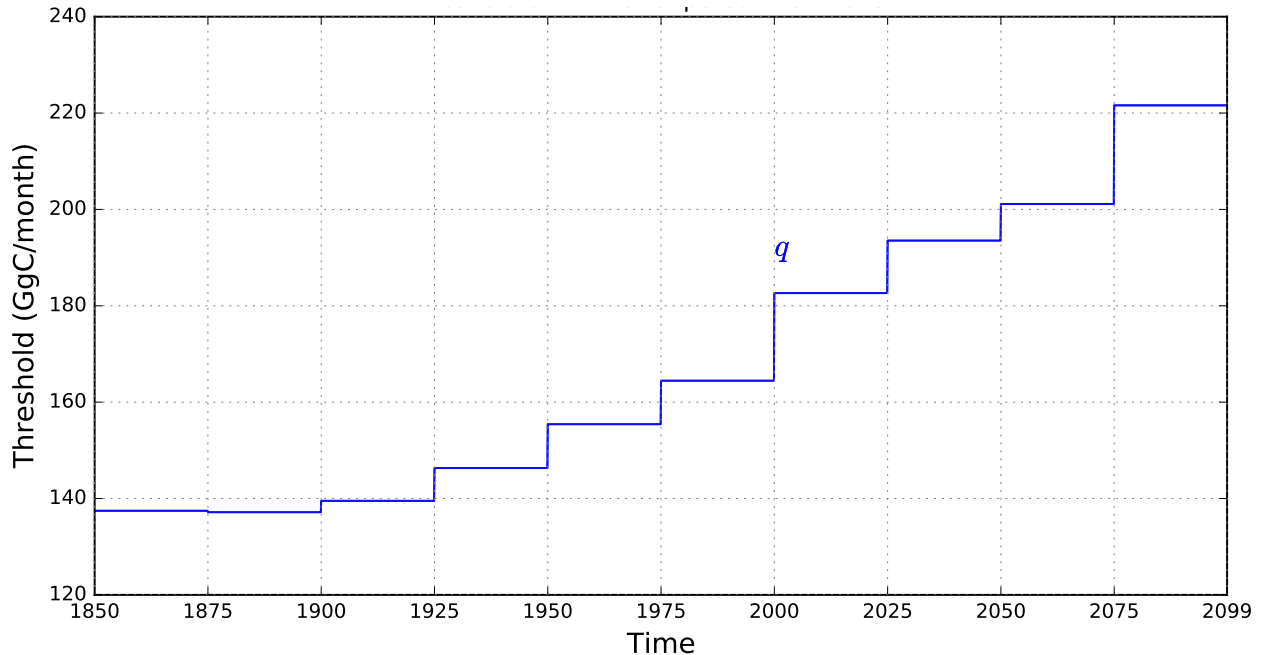
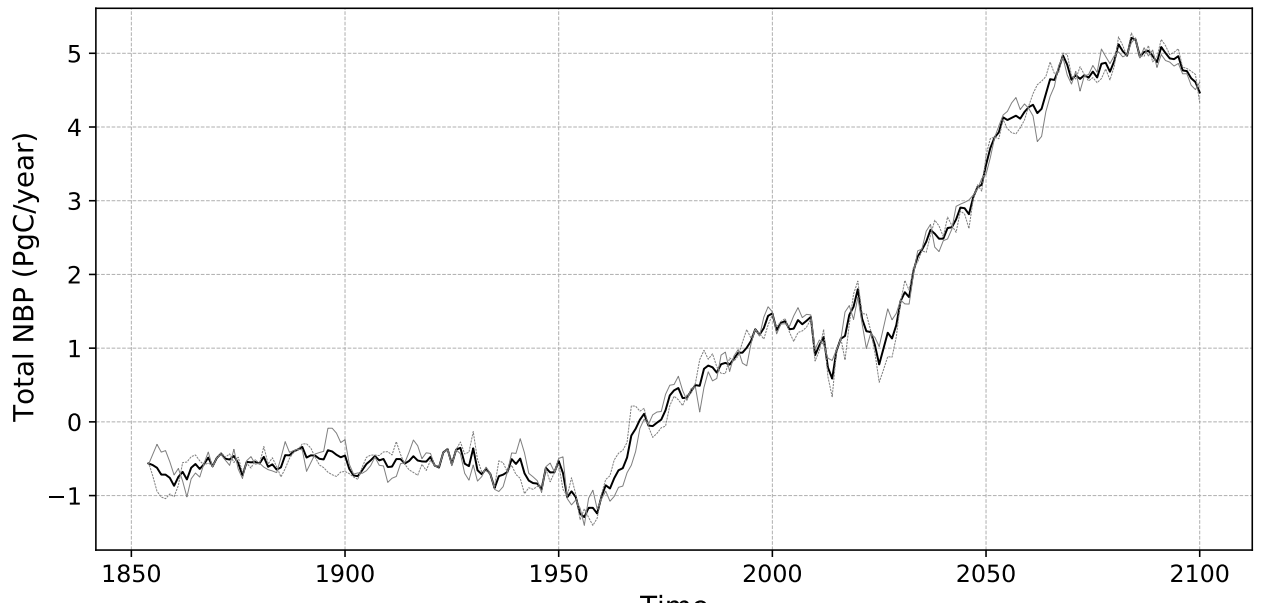


Figure S2. The spatial bounds of SREX reference regions defined by IPCC AR5. The abbreviations of the SREX regions (listed in Table S1) are shown within the bounds of that region.



(a)



(b)

Figure S3. (a) The 5th percentile threshold, q , of NBP anomalies based on a common percentile is represented by a blue line graph. The negative extremes in NBP are those NBP anomalies that are less than $-q$ and positive extremes are greater than q . (b) The global integrated 5 year rolling mean of NBP from 1850–2100 for CESM2 ensemble members (shown in gray) and mean of ensemble members (black).

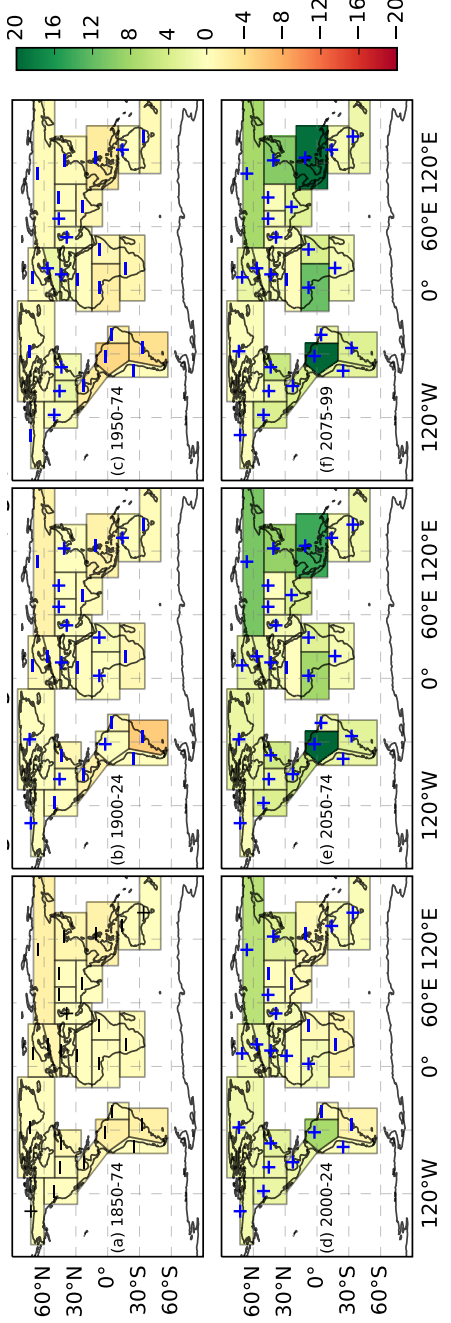
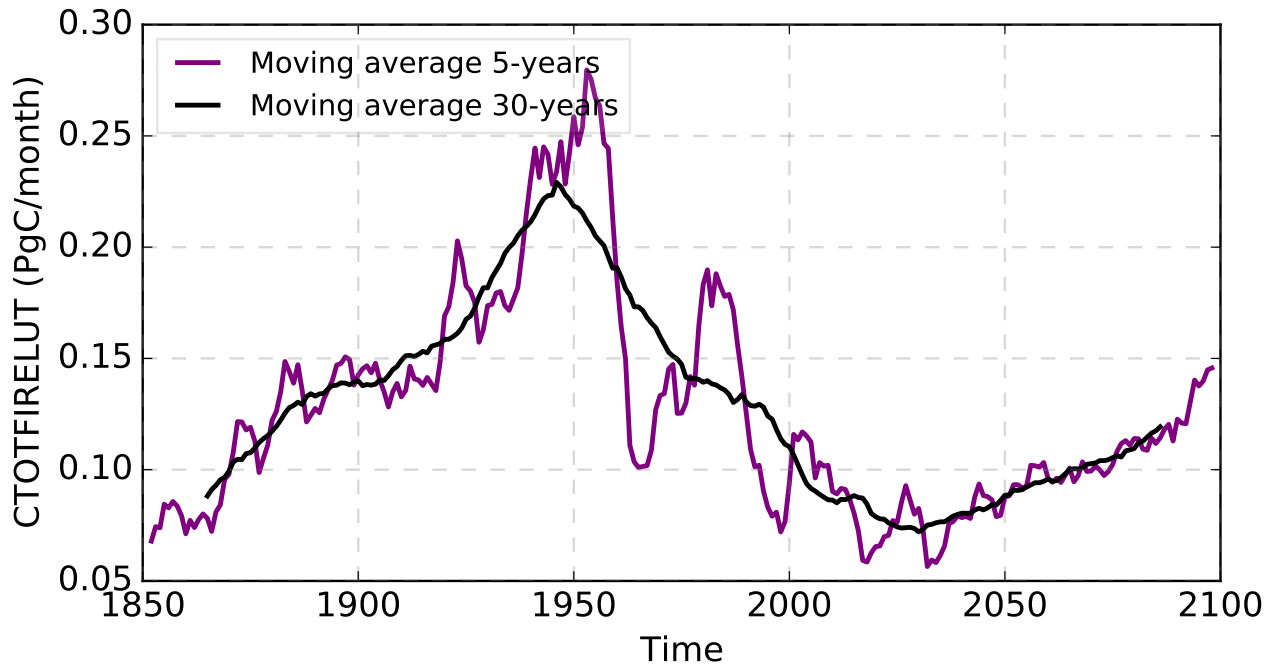
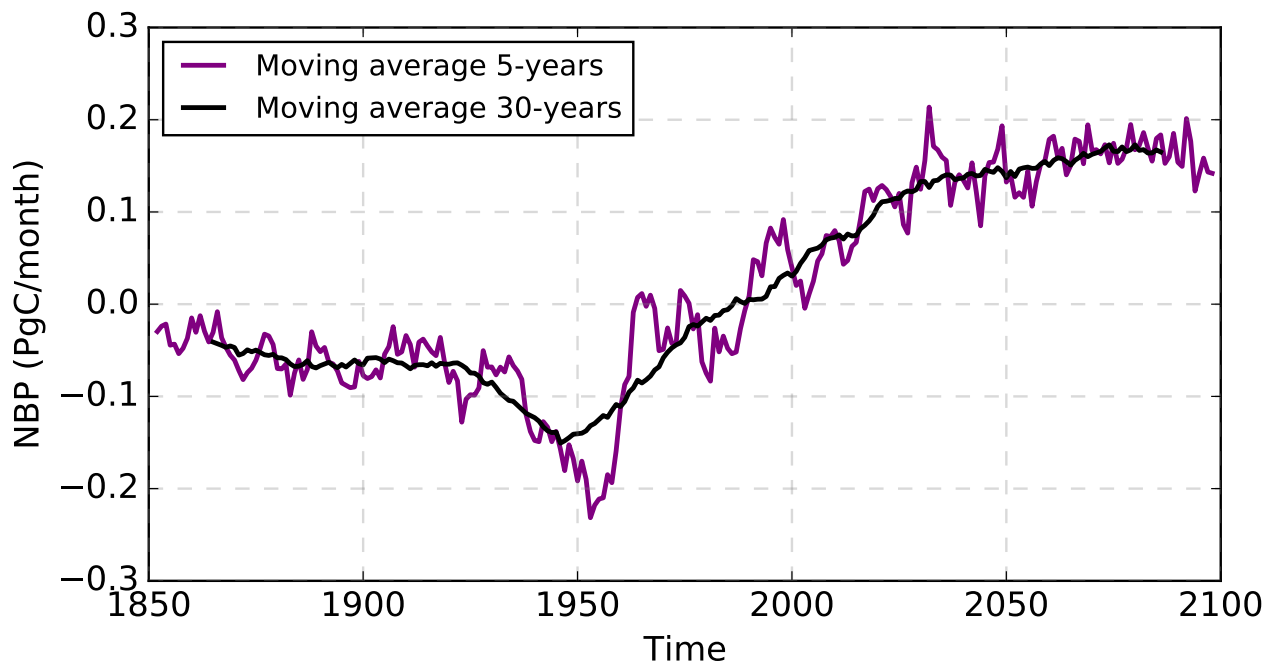


Figure S4. Total integral net biomass productivity (PgC) for 25 years time periods. The figure shows the changing spatial distribution of net uptake change (PgC) during following periods: (a) 1850–74, (b) 1900–24, (c) 1950–74, (d) 2000–24, (e) 2050–74, and (f) 2075–99. Net increase in regional NBP or total carbon uptake is represented by green color and '+' sign; net decrease is represented by red color and '-' sign.



(a)



(b)

Figure S5. (a) The global integrated 5 year and 30 year rolling mean of (a) total carbon loss from natural and managed fire of land-use grid cells (including deforestation fires) and (b) NBP from 1850 to 2100 for Central America (CAM). (a) The largest carbon loss was during the period of 1940–1960s. (b) The integrated NBP saturated around the year 2075 and it declines beyond 2075.

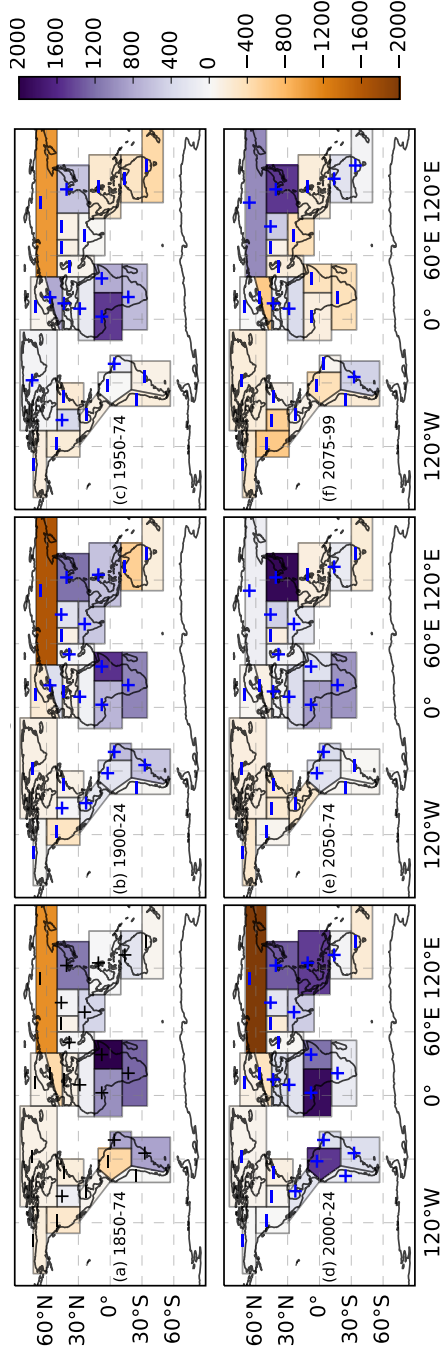


Figure S6. Spatial distribution of difference of count positive – negative NBP extreme events. Purple color ('+' sign) highlights the regions when positive exceed negative NBP extremes and brown color ('-' sign) shows regions when negative exceed positive NBP extremes. Towards the end of 21st century, most tropical regions are dominated by the frequency of negative extremes.

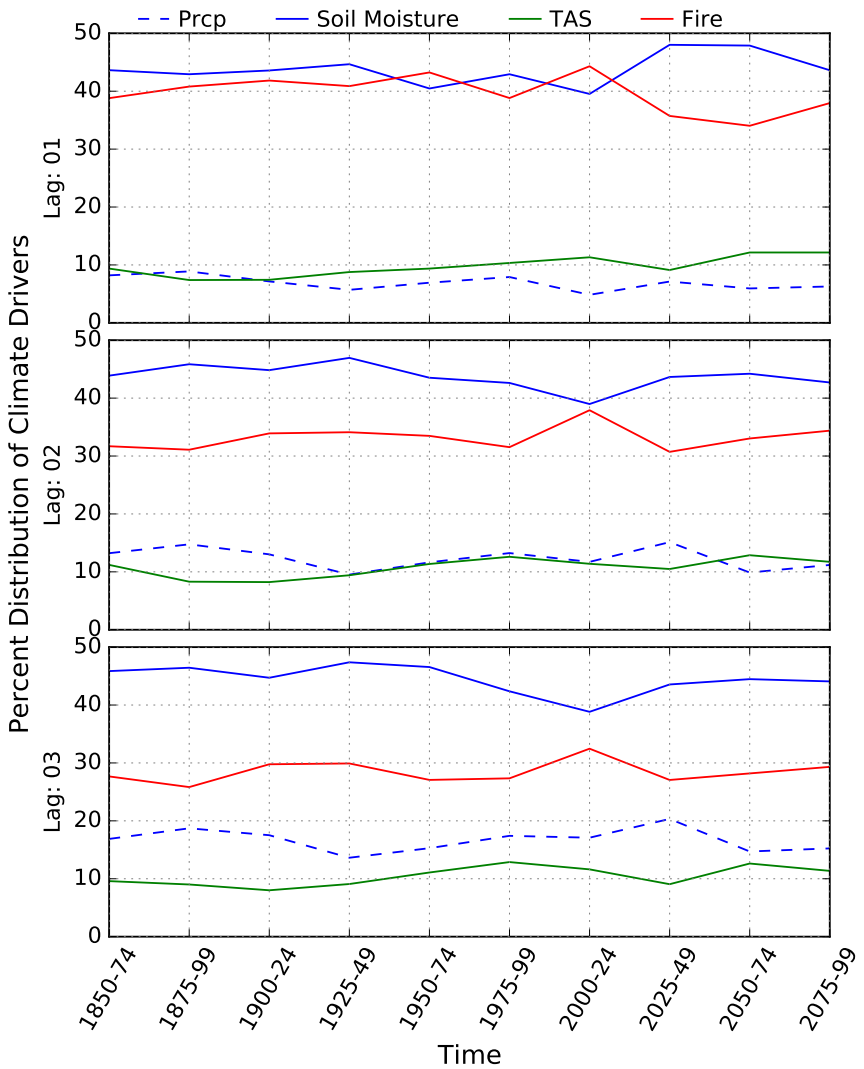
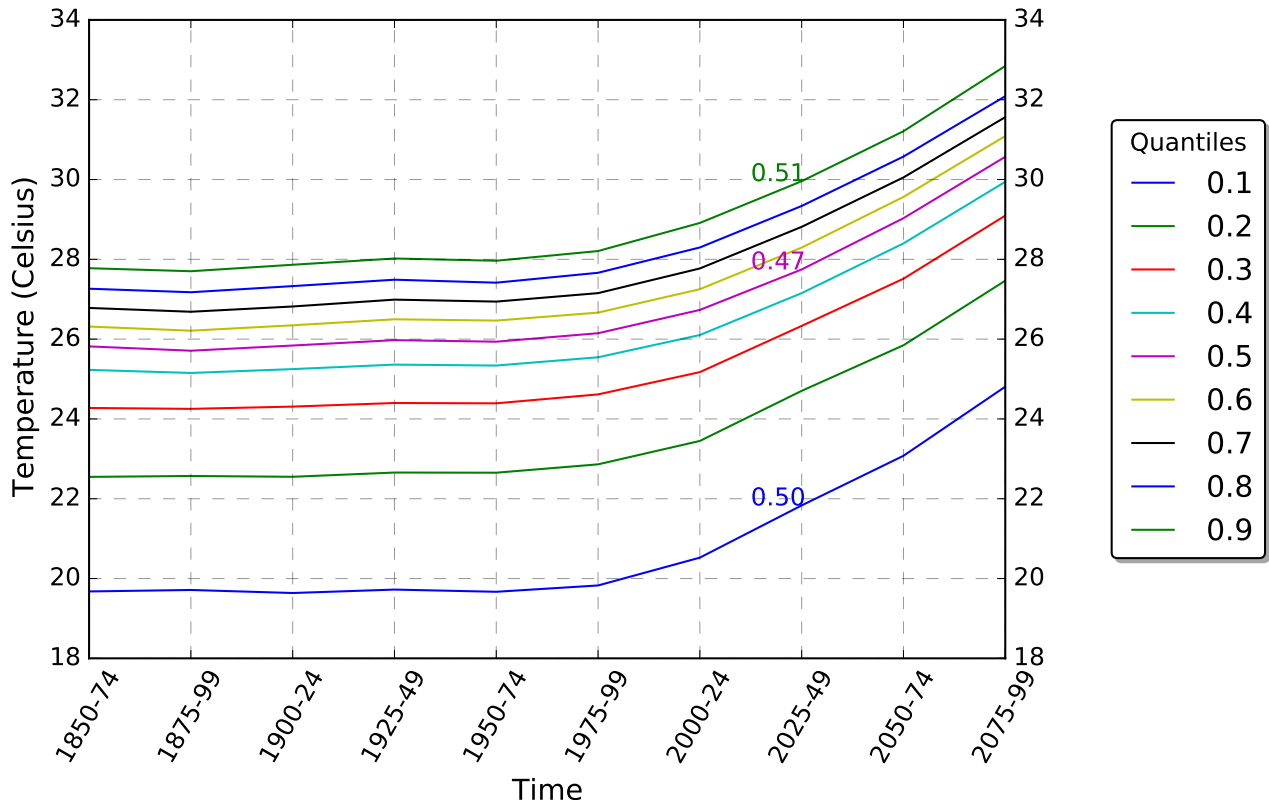
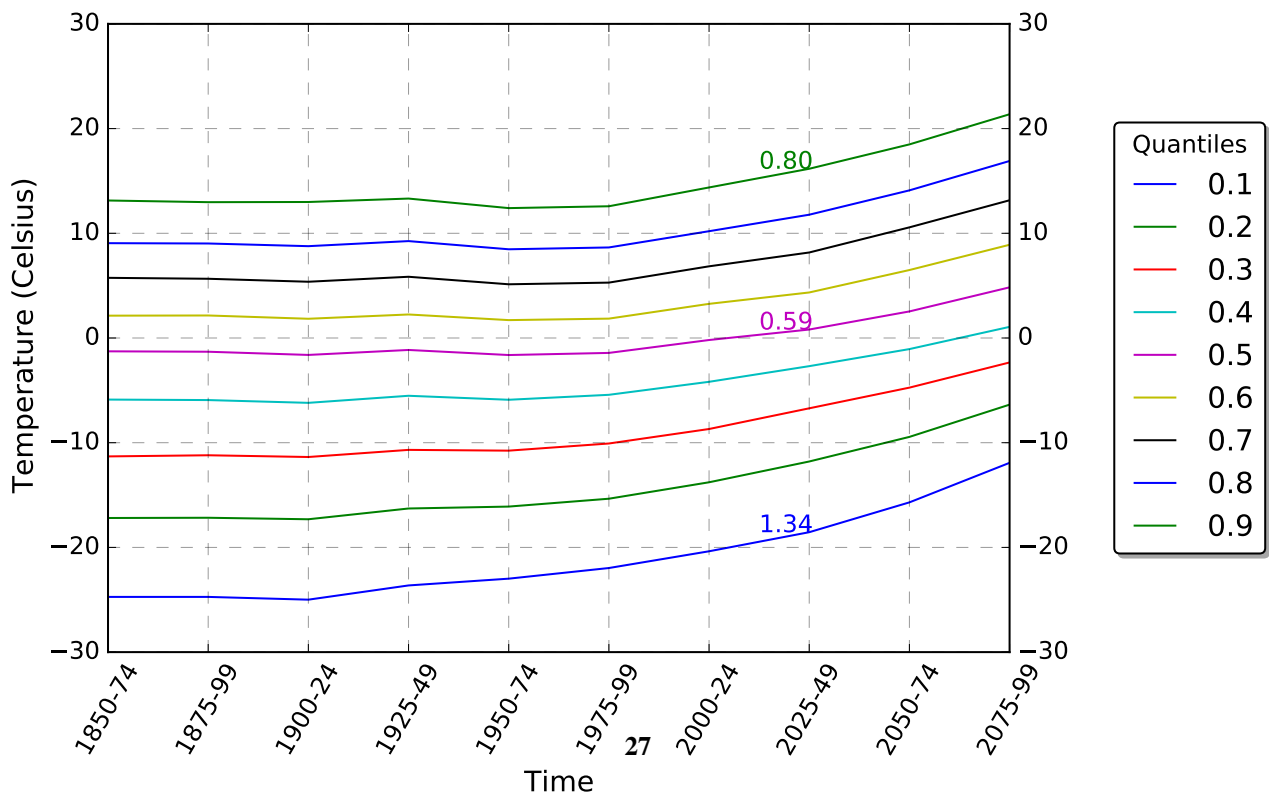


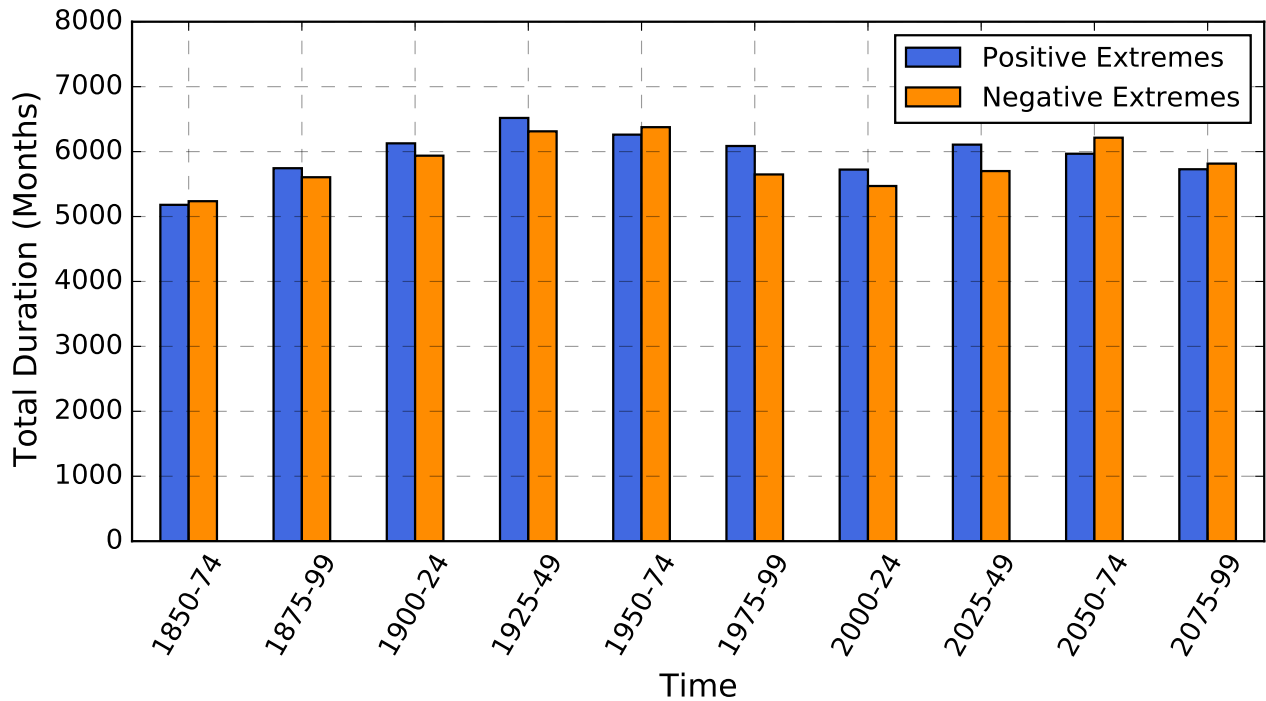
Figure S7. Percent distribution of count of dominant climate drivers causing time continuous carbon cycle extremes from 1850 to 2100 for every 25 year period. The dominance of climate drivers is estimated by the absolute magnitude of correlation coefficient ($p < 0.05$) at lags of 1 (top), 2 (middle), and 3 (bottom) months.



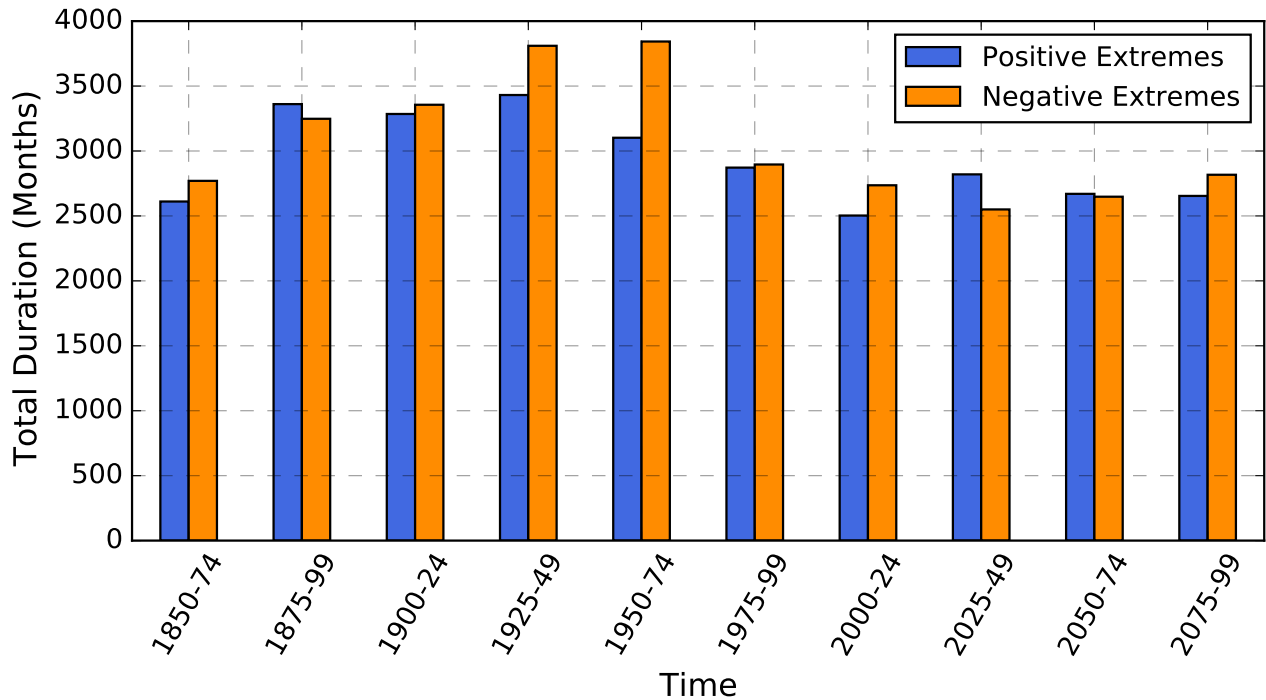
(a)



(b)



(a)



(b)

Figure S9. (a) The total duration of negative and positive NBP extremes in the region of Central America (CAM). The largest carbon emission from land use change occurred around 1950, which is also dominated by net negative carbon cycle extremes. The periods from 2050 onward shows net increase in the net negative extremes in NBP. (b) The total duration of negative and positive NBP extremes in the

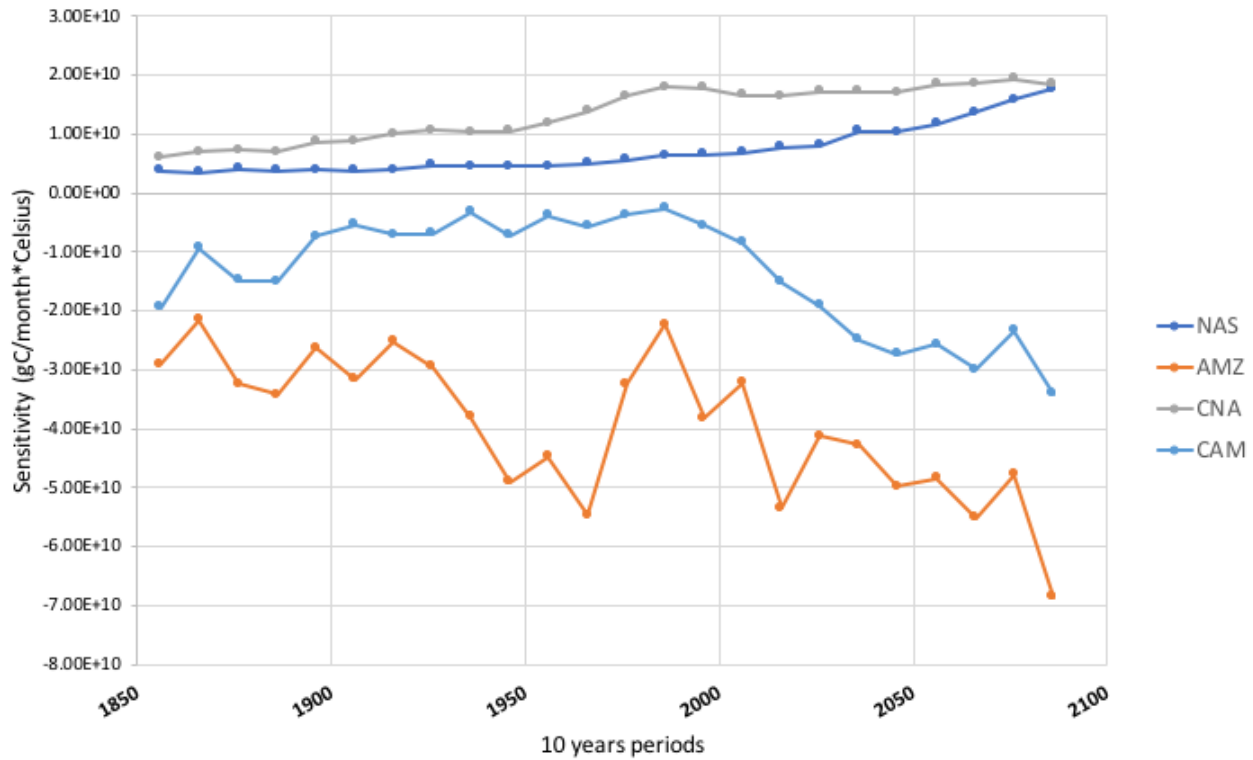


Figure S10. Changing temperature sensitivity of detrended anomalies in NBP to detrended anomalies in surface temperature for 10 year time periods at multiple SREX regions. The regions at higher latitudes have positive NBP sensitivity to temperature anomalies and low latitudes have negative sensitivity, and both sensitivities are strengthening over time.

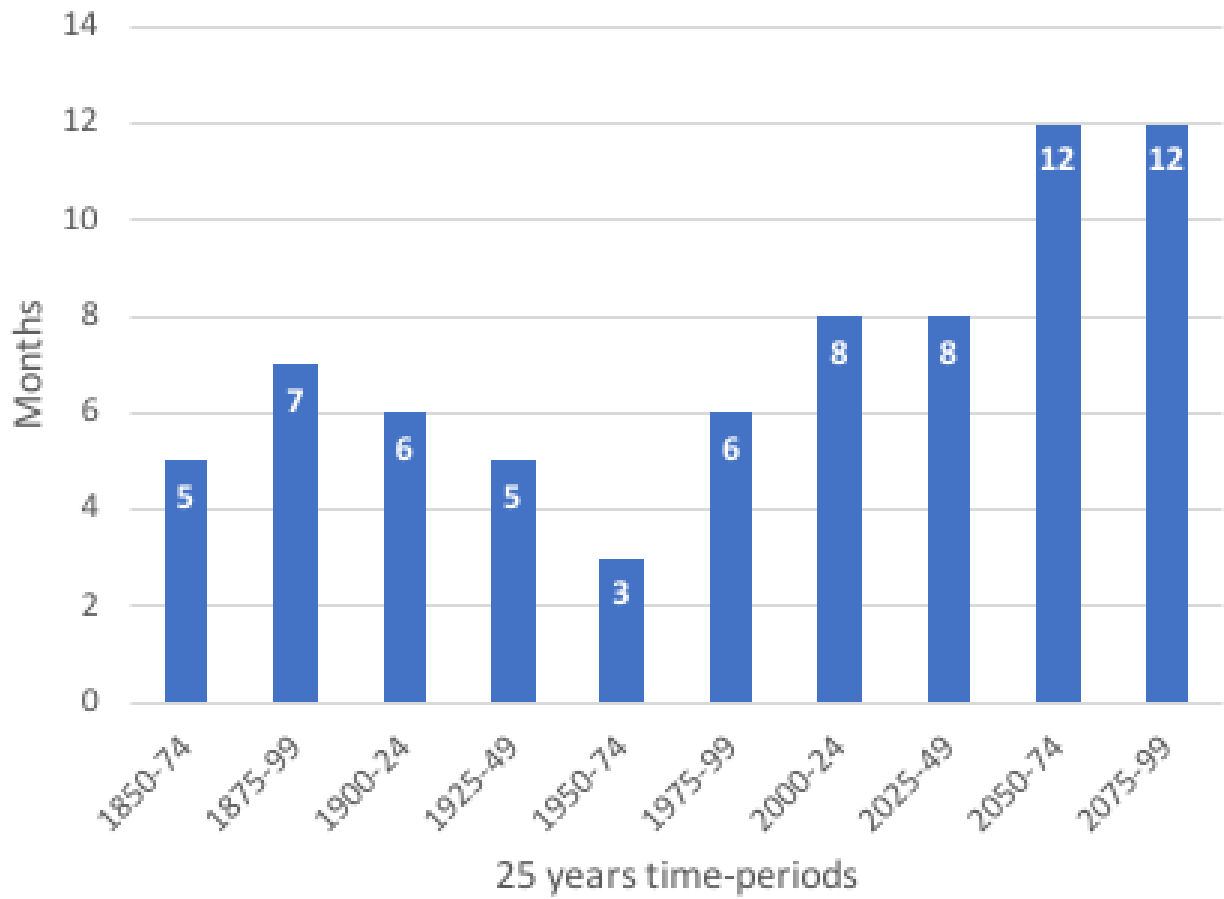


Figure S11. Concurrency at a lag of 2 months of temperature (90th % quantile and higher) and low NBP (10th % quantile and lower) at 51.36° North and 113.75° East in Northern Asia. The number of common months of hot temperatures and low NBP are shown at the top of every 25 year period bar chart.

Table S1. SREX Reference Regions

Abreviation	Region's Full Name
ALA	Alaska/N.W. Canada
AMZ	Amazon
CAM	Central America/Mexico
CAS	Central Asia
CEU	Central Europe
CGI	Canada/Greenland/Iceland
CNA	Central North America
EAF	East Africa
EAS	East Asia
ENA	East North America
MED	South Europe/Mediterranean
NAS	North Asia
NAU	North Australia
NEB	North-East Brazil
NEU	North Europe
SAF	Southern Africa
SAH	Sahara
SAS	South Asia
SAU	South Australia/New Zealand
SEA	Southeast Asia
SSA	Southeastern South America
TIB	Tibetan Plateau
WAF	West Africa
WAS	West Asia
WNA	West North America
WSA	West Coast South America

Author contributions. BS designed the experiment with inputs from JK, FH, and AG. FH arranged for the funding of the project. BS performed the experiment, data analysis, and wrote the manuscript with input from all co-authors.

Competing interests. The authors declare that they have no conflict of interest.

410 *Acknowledgements.* This research was supported by the Reducing Uncertainties in Biogeochemical Interactions through Synthesis and
Computation (RUBISCO) Science Focus Area, which is sponsored by the Regional and Global Model Analysis (RGMA) activity of the
Earth & Environmental Systems Modeling (EESM) Program in the Earth and Environmental Sciences Sciences Division (EESD) of the
Office of Biological and Environmental Research (BER) in the US Department of Energy Office of Science. This research used resources of
the National Energy Research Scientific Computing Center (NERSC), a U.S. Department of Energy Office of Science User Facility located
415 at Lawrence Berkeley National Laboratory, operated under Contract No. DE-AC02-05CH11231 for the Project m2467.

References

- Ault, T. R.: On the essentials of drought in a changing climate, *Science*, 368, 256–260, <https://doi.org/10.1126/science.aaz5492>, 2020.
- Bonan, G.: *Ecological Climatology: Concepts and Applications*, Cambridge University Press, 3 edn., <https://doi.org/10.1017/CBO9781107339200>, 2015.
- 420 Danabasoglu, G., Lamarque, J.-F., Bacmeister, J., Bailey, D. A., DuVivier, A. K., Edwards, J., Emmons, L. K., Fasullo, J., Garcia, R., Gettelman, A., Hannay, C., Holland, M. M., Large, W. G., Lauritzen, P. H., Lawrence, D. M., Lenaerts, J. T. M., Lindsay, K., Lipscomb, W. H., Mills, M. J., Neale, R., Oleson, K. W., Otto-Bliesner, B., Phillips, A. S., Sacks, W., Tilmes, S., van Kampenhout, L., Vertenstein, M., Bertini, A., Dennis, J., Deser, C., Fischer, C., Fox-Kemper, B., Kay, J. E., Kinnison, D., Kushner, P. J., Larson, V. E., Long, M. C., Mickelson, S., Moore, J. K., Nienhouse, E., Polvani, L., Rasch, P. J., and Strand, W. G.: The Community Earth System Model Version 2 (CESM2), *Journal of Advances in Modeling Earth Systems*, 12, e2019MS001916, <https://doi.org/10.1029/2019MS001916>, e2019MS001916 2019MS001916, 2020.
- Diffenbaugh, N. S., Singh, D., Mankin, J. S., Horton, D. E., Swain, D. L., Touma, D., Charland, A., Liu, Y., Haugen, M., Tsiang, M., and Rajaratnam, B.: Quantifying the influence of global warming on unprecedented extreme climate events, *Proceedings of the National Academy of Sciences*, 114, 4881–4886, <https://doi.org/10.1073/pnas.1618082114>, 2017.
- 430 Flach, M., Brenning, A., Gans, F., Reichstein, M., Sippel, S., and Mahecha, M. D.: Vegetation modulates the impact of climate extremes on gross primary production, *Biogeosciences Discussions*, 2020, 1–20, <https://doi.org/10.5194/bg-2020-80>, 2020.
- Frank, D., Reichstein, M., Bahn, M., Thonicke, K., Frank, D., Mahecha, M. D., Smith, P., van der Velde, M., Vicca, S., Babst, F., Beer, C., Buchmann, N., Canadell, J. G., Ciais, P., Cramer, W., Ibrom, A., Miglietta, F., Poulter, B., Rammig, A., Seneviratne, S. I., Walz, A., Wattenbach, M., Zavala, M. A., and Zscheischler, J.: Effects of climate extremes on the terrestrial carbon cycle: concepts, processes and potential future impacts, *Global Change Biology*, 21, 2861–2880, <https://doi.org/10.1111/gcb.12916>, 2015.
- 435 Friedlingstein, P., Jones, M., O’sullivan, M., Andrew, R., Hauck, J., Peters, G., Peters, W., Pongratz, J., Sitch, S., Le Quéré, C., et al.: Global carbon budget 2019, *Earth System Science Data*, 11, 1783–1838, 2019.
- Golyandina, N., Nekrutkin, V., and Zhigljavsky, A. A.: *Analysis of Time Series Structure: SSA and Related Techniques*, Chapman and Hall/CRC, 1 edn., <https://doi.org/10.1201/9781420035841>, 2001.
- 440 Grose, M. R., Narsey, S., Delage, F. P., Dowdy, A. J., Bador, M., Boschat, G., Chung, C., Kajtar, J. B., Rauniyar, S., Freund, M. B., Lyu, K., Rashid, H., Zhang, X., Wales, S., Trenham, C., Holbrook, N. J., Cowan, T., Alexander, L., Arblaster, J. M., and Power, S.: Insights From CMIP6 for Australia’s Future Climate, *Earth’s Future*, 8, e2019EF001469, <https://doi.org/10.1029/2019EF001469>, e2019EF001469 2019EF001469, 2020.
- Hubau, W., Lewis, S. L., Phillips, O. L., Affum-Baffoe, K., Beeckman, H., Cuní-Sánchez, A., Daniels, A. K., Ewango, C. E., Fauset, S., Mukinzi, J. M., et al.: Asynchronous carbon sink saturation in African and Amazonian tropical forests, *Nature*, 579, 80–87, <https://doi.org/10.1038/s41586-020-2035-0>, 2020.
- 445 Langenbrunner, B., Pritchard, M. S., Kooperman, G. J., and Randerson, J. T.: Why Does Amazon Precipitation Decrease When Tropical Forests Respond to Increasing CO₂?, *Earth’s Future*, 7, 450–468, <https://doi.org/10.1029/2018EF001026>, 2019.
- Lawrence, D. M., Fisher, R. A., Koven, C. D., Oleson, K. W., Swenson, S. C., Bonan, G., Collier, N., Ghimire, B., van Kampenhout, L., Kennedy, D., et al.: The Community Land Model version 5: Description of new features, benchmarking, and impact of forcing uncertainty, *Journal of Advances in Modeling Earth Systems*, 11, 4245–4287, 2019.

- Li, F., Levis, S., and Ward, D. S.: Quantifying the role of fire in the Earth system; Part 1: Improved global fire modeling in the Community Earth System Model (CESM1), *Biogeosciences*, 10, 2293–2314, <https://doi.org/10.5194/bg-10-2293-2013>, 2013.
- Liu, L., Gudmundsson, L., Hauser, M., Qin, D., Li, S., and Seneviratne, S. I.: Soil moisture dominates dryness stress on ecosystem production
455 globally, *Nature Communications*, 11, 1–9, 2020.
- Marcolla, B., Migliavacca, M., Rödenbeck, C., and Cescatti, A.: Patterns and trends of the dominant environmental controls of net biome productivity, *Biogeosciences*, 17, 2365–2379, <https://doi.org/10.5194/bg-17-2365-2020>, 2020.
- Pan, S., Yang, J., Tian, H., Shi, H., Chang, J., Ciais, P., Francois, L., Frieler, K., Fu, B., Hickler, T., Ito, A., Nishina, K., Ostberg, S., Reyer, C. P., Schaphoff, S., Steinkamp, J., and Zhao, F.: Climate Extreme Versus Carbon Extreme: Responses of Terrestrial Carbon Fluxes to Temperature and Precipitation, *Journal of Geophysical Research: Biogeosciences*, 125, e2019JG005252, <https://doi.org/10.1029/2019JG005252>, 2019.
- Piao, S., Zhang, X., Chen, A., Liu, Q., Lian, X., Wang, X., Peng, S., and Wu, X.: The impacts of climate extremes on the terrestrial carbon cycle: A review, *Science China Earth Sciences*, 62, 1551–1563, 2019.
- Reichstein, M., Bahn, M., Ciais, P., Frank, D., Mahecha, M. D., Seneviratne, S. I., Zscheischler, J., Beer, C., Buchmann, N., Frank, D. C.,
460 Papale, D., Rammig, A., Smith, P., Thonicke, K., van der Velde, M., Vicca, S., Walz, A., and Wattenbach, M.: Climate extremes and the carbon cycle, *Nature*, 500, 287–295, <https://doi.org/10.1038/nature12350>, 2013.
- Ribeiro, A. F. S., Russo, A., Gouveia, C. M., Páscoa, P., and Zscheischler, J.: Risk of crop failure due to compound dry and hot extremes estimated with nested copulas, *Biogeosciences*, 17, 4815–4830, <https://doi.org/10.5194/bg-17-4815-2020>, 2020.
- Seneviratne, S. I., Nicholls, N., Easterling, D., Goodess, C. M., Kanae, S., Kossin, J., Luo, Y., Marengo, J., McInnes, K., Rahimi, M., Reichstein, M., Sorteberg, A., Vera, C., and Zhang, X.: Changes in Climate Extremes and their Impacts on the Natural Physical Environment, pp. 109–230, Cambridge Univ. Press, Cambridge, U.K., and New York, [Field, C.B., V. Barros, T.F. Stocker, D. Qin, D.J. Dokken, K.L. Ebi, M.D. Mastrandrea, K.J. Mach, G.-K. Plattner, S.K. Allen, M. Tignor, and P.M. Midgley (eds.)]. A Special Report of Working Groups I and II of the Intergovernmental Panel on Climate Change (IPCC), 2012.
- Turetsky, M. R., Abbott, B. W., Jones, M. C., Anthony, K. W., Olefeldt, D., Schuur, E. A., Grosse, G., Kuhry, P., Hugelius, G., Koven, C.,
475 et al.: Carbon release through abrupt permafrost thaw, *Nature Geoscience*, 13, 138–143, 2020.
- von Buttlar, J., Zscheischler, J., Rammig, A., Sippel, S., Reichstein, M., Knohl, A., Jung, M., Menzer, O., Arain, M. A., Buchmann, N., Cescatti, A., Gianelle, D., Kiely, G., Law, B. E., Magliulo, V., Margolis, H., McCaughey, H., Merbold, L., Migliavacca, M., Montagnani, L., Oechel, W., Pavelka, M., Peichl, M., Rambal, S., Raschi, A., Scott, R. L., Vaccari, F. P., van Gorsel, E., Varlagin, A., Wohlfahrt, G., and Mahecha, M. D.: Impacts of droughts and extreme-temperature events on gross primary production and ecosystem respiration: a systematic assessment across ecosystems and climate zones, *Biogeosciences*, 15, 1293–1318, <https://doi.org/10.5194/bg-15-1293-2018>, 2018.
- Wu, Z., K. Schneider, E., Kirtman, B., Sarachik, E., Huang, N., and J. Tucker, C.: The modulated annual cycle: An alternative reference frame for climate anomalies, *Climate Dynamics*, 31, 823–841, <https://doi.org/10.1007/s00382-008-0437-z>, 2008.
- Zhang, T., Xu, M., Xi, Y., Zhu, J., Tian, L., Zhang, X., Wang, Y., Li, Y., Shi, P., Yu, G., Sun, X., and Zhang, Y.: Lagged climatic effects on
485 carbon fluxes over three grassland ecosystems in China, *Journal of Plant Ecology*, 8, 291–302, <https://doi.org/10.1093/jpe/rtu026>, 2014.
- Zscheischler, J., Mahecha, M. D., von Buttlar, J., Harmeling, S., Jung, M., Rammig, A., Randerson, J. T., Schölkopf, B., Seneviratne, S. I., Tomelleri, E., Zaehle, S., and Reichstein, M.: A few extreme events dominate global interannual variability in gross primary production, *Environmental Research Letters*, 9, 035 001, <https://doi.org/10.1088/1748-9326/9/3/035001>, 2014.

Zscheischler, J., Westra, S., Van Den Hurk, B. J., Seneviratne, S. I., Ward, P. J., Pitman, A., Aghakouchak, A., Bresch, D. N., Leonard, M.,

490 Wahl, T., and Zhang, X.: Future climate risk from compound events, *Nature Climate Change*, 8, 469–477, <https://doi.org/10.1038/s41558-018-0156-3>, 2018.